INTEGRATED STUDY FOR HYDROCARBON ACCESSMENT OF JOYA MAIR AREA UPPER INDUS BASIN PAKISTAN USING 2D SEISMIC DATA AND WELL LOGS

BY

Mohsin Ali Khan

BS Geophysics

2016-2020

Department of Earth Sciences

Quaid-i-Azam University Islamabad

TO Allah belongs all that is in the heavens and all that is on the earth, and whether you disclose what is in your ownselves or conceal it, Allah will call you to account for it. Then He forgive whom He wills and punishes whom He wills. and Allah is Able to do all things. (surah Al-Baqarah)

CERTIFICATE

This dissertation submitted by **MOHSIN ALI KHAN** s/o **ARSHAD HUSSAIN** is accepted in its present form by the Department of Earth Sciences, Quaid-i-Azam University Islamabad as satisfying the requirement for the award of bachelor's degree in Geophysics.

RECOMMENDED BY

Dr. ABBAS ALI NASEEM: _____
(*Supervisor)*

Dr. AMIR ALI: _____
(Chairperson Department of Earth Sciences)

EXTERNAL EXAMINER: _____

DEDICATED

TO

MY BELOVED PARENTS,

TEACHERS AND FRIENDS.

ACKNOWLEDGEMENT

In the name of Allah the most merciful and most beneficent. All praises to him who is Almighty, The One, The Everlasting, Who begets none, is begotten, by no one, and there is none His equal. O' God I am really thankful to you that you make me capable to complete my work. I am nothing without your help. Please keep me always in prostration before you and let me not leave before anyone except you.

I am especially thankful to my dissertation supervisor **Dr. ABBAS ALI NASEEM** that he always gave me his loving guidance whenever I asked and spared His precious time for me during my work. I extremely grateful to all my teachers for their endless love, prayers and encouragements Dr.Amir Ali, Dr.Faisal, Dr Shazia Asim ,Dr Anees Bangash, Dr Tahir Azeem and I inspired throughout my degree at QAU.

I am thankful to my respectable friend and senior, Zahid ullah khan, M Ishaq Mr Hamza for his corporation and guidance in every aspect of life not only in thesis work.

MOHSIN ALI KHAN
GEOPHYSICS
Q.A.U. ISLAMABAD

Contents

Abstract

The JoyaMair is oil field located in the south-southeast part of salt Range-PotwarForland Basin. It comprises the structures that result from the compressional tectonic regime. The main structure includes thrust and back thrust anticline as a result of collision between Indian and Eurasian plate. For the hydrocarbon accumulation these structures are important if proper petroleum play is available. The structure of the area is delineated with the help of four (4) dip lines and two (2) crosslines. A triangular zone is marked on the seismic lines which act as suitable trap for petroleum play and Minwal X-1 well is drilled on the structure. The main reservoir of the area is Chorgali Formation and Skasser limestone of Eocene age. To evaluate the hydrocarbon potential in the reservoir an integrated geophysical and petorphysical study is done. Petrophysical study shows a good percentage of effective porosity 13% in both of the reservoirs with Hydrocarbon saturation upto 68%. Seismic attributes highlighted the potential zones in the reservoir and Colored inversion shows the elastic property i.e. Impedance of the reservoir suitable for hydrocarbon.

CHAPTER 01: INTRODUCTION TO STUDY AREA

1.1 Introduction:

The Upper Indus Potwar sub-basin is located in the sub-Himalayan land and contains a large number of structural traps created as a result of Tertiary Himalayan thrusting and folding. It consists of Potwar plateau, the Salt Range and the Jhelum Plains. The geological arrangement of the Potwar Basin is a roughly complex structure of the hand one is dealt which is the result of the Tertiary Himalayan collision between Eurasian and Indian plates. The Potwar sub-basin is filled with thick Pre-Cambrian evaporates overlain by relatively thin platform deposits of Cambrian to Eocene age followed by thick Miocene-Pliocene molasses. This whole section has been deformed by intensive Himalayan orogeny in Pliocene to Middle Pleistocene.

In this basin have oil dominant. Eocene and Paleocene reservoirs are the most productive reservoirs in different areas. The eastern Potwar have one of the most productive zones in this area. The Potwar sub-basin is one of the oldest oil provinces of the world, where the first commercial discovery was made in 1914 at Khaur In the area, 396 wells have been drilled but many of these were pre-maturely desolate, as these could not do their propose depth right to drilling problems discussion to high brought pressure to bear up on water in molasses deposits, which may be related to structural complexities (Moghul et al., 2007).

In the salt range it has March to a disparate drummer structural style. Uneven distribution of caustic soda, risk of different detachment levels, faults and flexures in the floor are in the applicable reasons for structural complexity. The Jhelum left alongside strike-slip fault in the east and the what is coming to one lateral strike-slip Kalabagh fault in the west have played important role in shaping the geometry of the Potwar sub-basin. This results in the outset of structural styles and hydrocarbon potential in the Potwar sub- basin.

1.2 Study area location:

The Joya Mair area is located round about 90 km South of Islamabad. The area can be easily accessed through Kashmir highway and motorway M2 (Islamabad-

Lahore), take an exit towards Talagang Chakwal road. At the first round about take the first exit onto Chakwal 5 bypass than further on the road take the first left at the Thanil Chowk onto the Thanil road; going further for 1 km we have Joya Mair.

Joya Mair area is in Jhelum, Punjab, and Pakistan. It is situated in the upper Indus basin. It lies in the south of Himalayan and Karakoram Mountains in the north of Pakistan. This area was situated due to the close attention forces. The diamond in the rough area is enclosed individually Longitude 32º 59′ 52″ N to 32º 99′ 80″ N and free hand Latitude 72º 49′ 31″ E to 72º 82′ 31″E

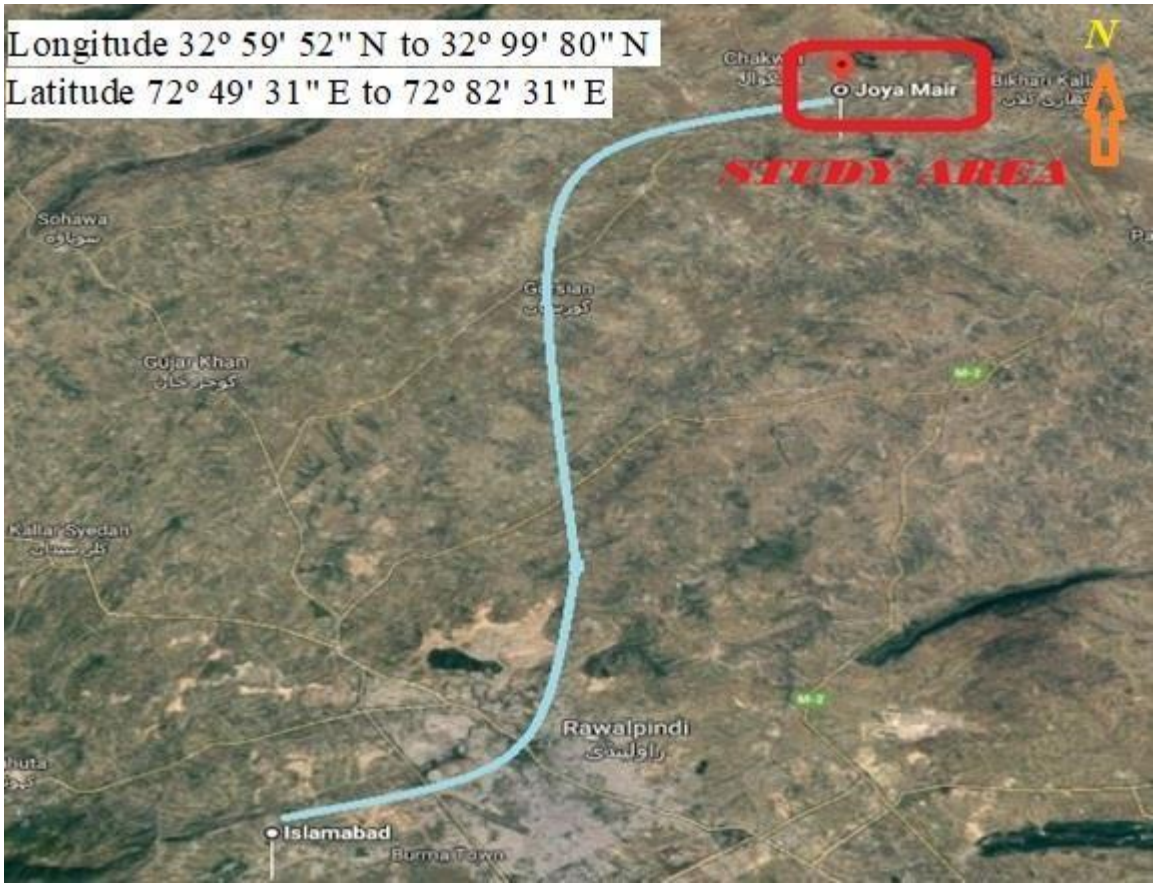

Fig 1.1: Study area location (Google Earth)

1.3 Upper Indus Basin Exploration History:

In the Upper Indus basin Petroleum exploration in Pakistan began with drilling of first well in 1866 at Kundal, Mianwali. Petroleum Exploration history of the Potwar Basin starts huge quantities of oil were discovered in 1915 at Khaur, district Attock, Punjab by the predecessor of Attock Oil Company (AOC). As a result of the combined efforts of AOC and Burma Oil Company (BOC), Dhulian (1936), Joya

Mair (1944) ,Balkassar (1946) and Toot (1968). During this period Pakistan Oil Limited (POL) discovered oil at Meyal (1968). Oil fields were discovered in the Potwar area establishing the oil potential of Potwar region. Occidental reported the most prolific discovery at Dhurnal-1 in Potwar region in 1984. The discovery of condensate/gas and oil at Dakhni (1983 and Dhurnal 1984) provided new leads to the hydrocarbon potential of Northern Potwar regions. Oxy discovered oil at Bhangali and Pindori during 1989-1990 in their Soan Concession. Pindori-1 during recompletion blows out and the well had to be abandoned but Pindori-2, 3, 4,5A and 6 are producing. OGDCL discovered heavy crude at Chak Naurang (1986), rested old Qazian Structure and found oil at Missa Keswal-1 (1990). Oil was also discovered by OGDC in Potwar at Sadkal (1991) near Fatehjang, Rajian (1993) and Kal (1995) near Chakwal. Other significant discoveries were made by POL at Pariwali-1 (sidetrack in 1986) and Turkwal-1 (sidetrack in 1997) wells in Ahmadal and Central Potwar Concessions (Zaidi et al., 2013).

OIL & GAS DEVELOPMENT LIMITED OGDCL make a breakthrough when oil was discovered for the first time in Kohat region at Chanda (former Shakardara Structure) from Datta Formation of Early Jurassic. As a matter of fact, this was first ever hydrocarbon discovery in KPK province which was followed by another discovery namely Manzalai (2002) and Makori (2005) by MOL of Hungary making Kohat plateau, new focus area for exploration. The discovery of Mela oil/gas (2006) by OGDCL, which were reinforced the belief of many Geologist that this region can host large hydrocarbon reserves with upside touching tens of trillion cubic feet of gas (Zaidi et al., 2013).

1.4 Data Formats:

The final migrated seismic section along with supportive data and petrophysical data obtained in following formats.

Types of	Form
Petrophysics	LAS
Seismic	SEG-Y
Seismic Velocities	VEL
Navigation	DAT
Well	LES
DEM	grid
Georeferenced satellite	grf, jpg

1.5 List of software tools and application:

- **Kingdom suit.**
  - Seismic Interpretation.
  - Velocity and interpolation and modeling
  - Time Contouring.
  - Depth Contouring.
  - Well Correlation.
  - Conversion of RMS,interval and average velocities.
  - Kingdom used for Rock Physics and Engineering Properties.

1.6 Acquisition Parameters:

1.6.1 Data Record:

Recorded By	P.O.L
Party Number	Seismic party #7
Data recorded	1996

1.6.2 Seismic Source Description:

Energy Source	Dynamite
Charge Pattern	1 Hole
Average Charge Size	5 kg
Shot Point Interval	50 Meters

1.7 Data Recording Parameters:

System	SN388
Format	DMU*SEG D
Aliasing Filter	120 Hz
Notch Filter	Out
Field Sampling Interval	2 millisecond
Record Length	6 seconds
No. of Data Traces	120

1.8 Survey Parameters:

Spread	3075-125-*-125-3075
Group Interval	50 meters
Type Of Geophones	SM4

Geophone Code	0312
Group length	97.30 meters
Geophone Interval	2.78 meters

1.8 2D Seismic lines:

Sr.no	Line number	Line direction	Well Location
1	SPOL-93-MN-05	Dip (North-South)	
2	SPOL-93-MN-06	Dip (North-South)	
3	SPOL-93-MN-08	Dip (North-South)	MINWAL-X-1
4	SPOL-93-MN-09	Dip (North-South)	
5	SPOL-93-MN-10	Strike (East-West)	
6	SPOL-93-MN-11	Strike (East-West)	

1.9 Base Map:

Base map is the map on which primary data and interpretations can be plotted. The base map is an important component of interpretation, as it displays the spatial position of each picket of a seismic section. It also shows the spatial relationship of all seismic sections under consideration, their tie point locations and provides the framework for contouring. The base map of the area is generated using KINGDOM SUITE

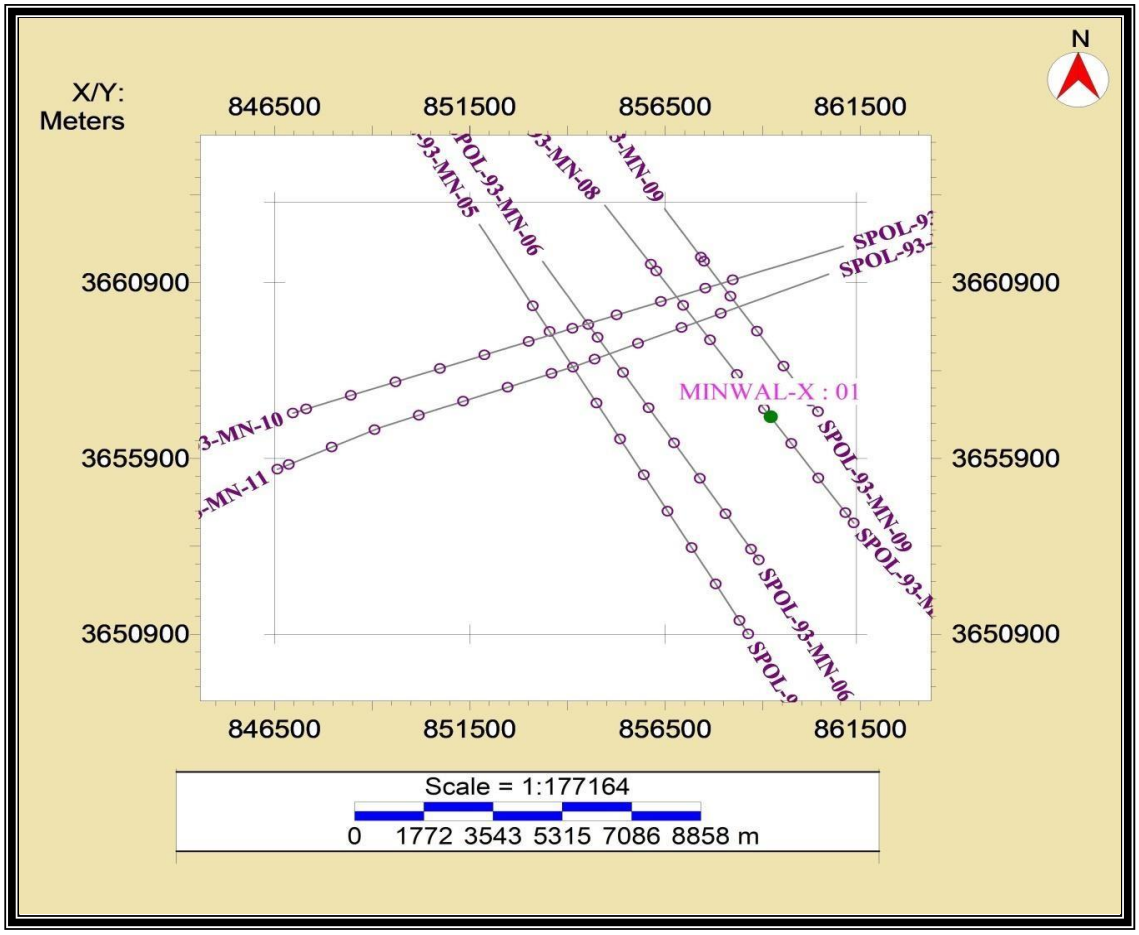

Fig.1.2. Base map of the study area showing the location of the seismic lines and Minwal X-1 wells.

1.10 Objective of Study:

The objectives of this study area:

- The Seismic data interpretation to delineate the subsurface structural geometry of the area. The describe of the subsurface structural and stratigraphic traps for hydrocarbon accumulations.
- Integration of seismic and well data to enhance the precision of the interpretation process.
- Conversion of interpreted time section into depth section to identify the depth of key horizons and to construct depth surface maps of the reservoir rocks.
- Seismic Attribute Analysis for the confirmation of the horizon marking
- Petrophysical analysis of the reservoirs present in the study area.

1.11 Methodology:

According to recent information that is under seismic facts and wells data of Minwal X-01 Base map of the concern area, seismic lines and well locations:

- Identify the exact location of horizons with the help of well data i.e. check shot and synthetic seismogram
- Time horizons are marked on the identified reflectors that form the petroleum play system.
- Time contour maps for the marked horizons are generated.
- Time to depth conversion is done with the help TD chart and velocity relation.
- Depth contour maps for the horizons are generated.
- Petrophysics is performed for the Saturation of water and hydrocarbon in the reservoir.
- Gassman fluid substation is applied to study the effects of fluid at the reservoir level.

CHAPTER 02: INTRODUCTION TO GENERAL GEOLOGY OF AREA

2.1 Introduction

The information about the geology of an area plays an important role for precise interpretation of seismic data. The interpretation of seismic data in geological terms is the objective of seismic project. Therefore seismic data interpretation is based on the stratigraphy and structural geology of the area. So as if we don't know geological formations in area, we don't recognize the different reflections appearing in the seismic section. This chapter deals with a brief description of the tectonic setting, structural geology and stratigraphy of the study area (Joya mair) and adjoining areas of upper Indus Basin.

2.2 Regional Geology and tectonic setting:

The upper Indus Basin the Potwar sub-basin is located in the western foothills of Himalayas in northern Pakistan. It consists of Potwar plateau, the Salt Range and the Jhelum Plains. It is bounded by MBT in the north, Salt range in south, Jhelum strike slip fault in the East and Kalabagh strike slip fault in the west. The general geology of SRPFB is over 6100 m of rocks ranging from Infra-Cambrian to Recent. The Potwar plateau comprises of less internally deformed fold and thrust belt having width of approximately 150 km in N-S direction. It comprises of thick Pre Cambrian evaporates overlain by thin platform deposits of Cambrian to Eocene rocks followed by thick Miocene-Pliocene molasses. The whole section has been subjected to intense Himalayan orogeny in Pliocene to Pleistocene. The Jhelum left lateral strike fault in the east and Kalabagh right lateral strike slip fault have played a vital role in shaping the geometry of Potwar sub-basin, drifting the basin towards south

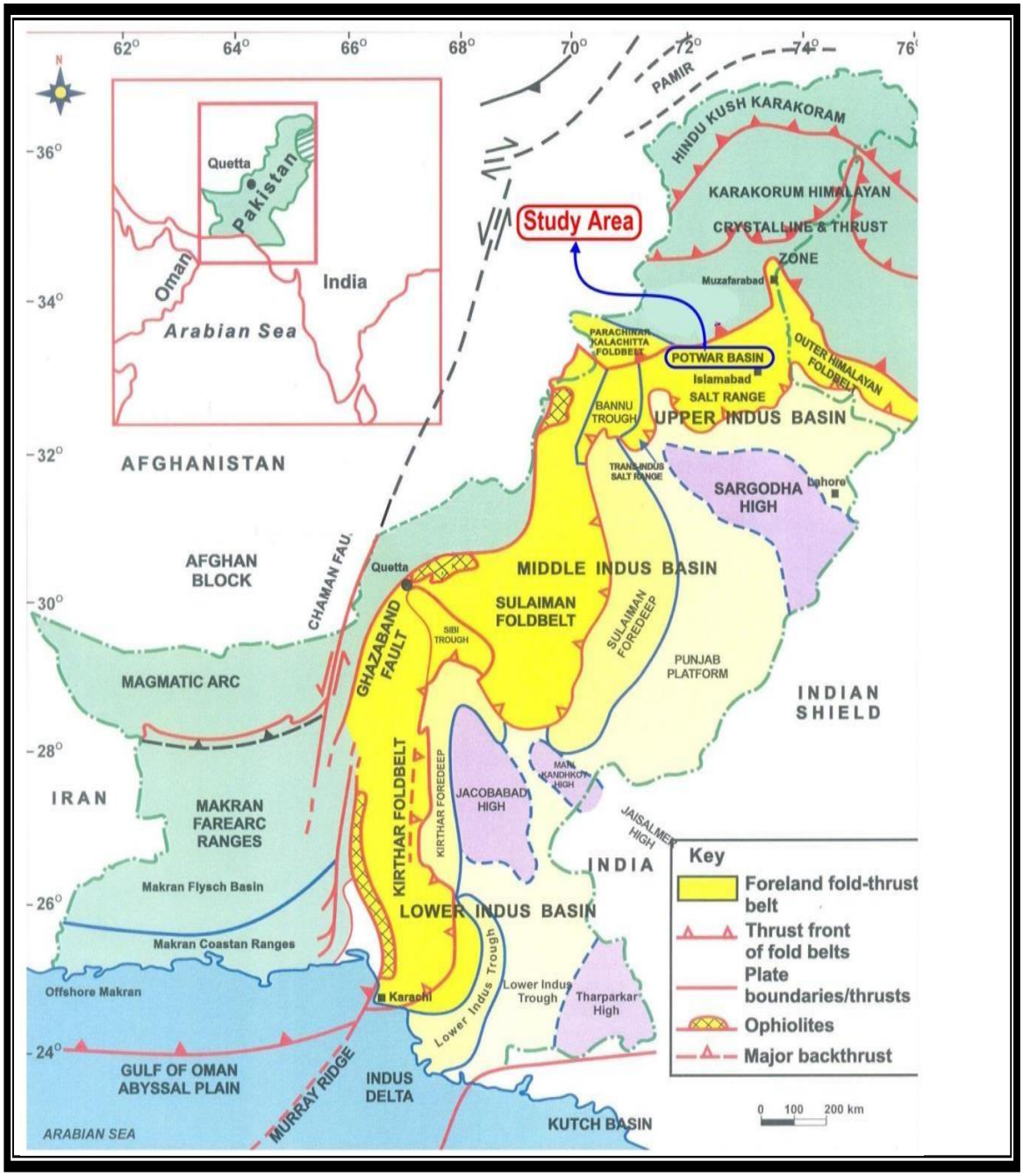

Fig 2.1. Map Showing location of study area with respect to Islamabad and its geological boundaries (Banks and Warburton, 1986).

.

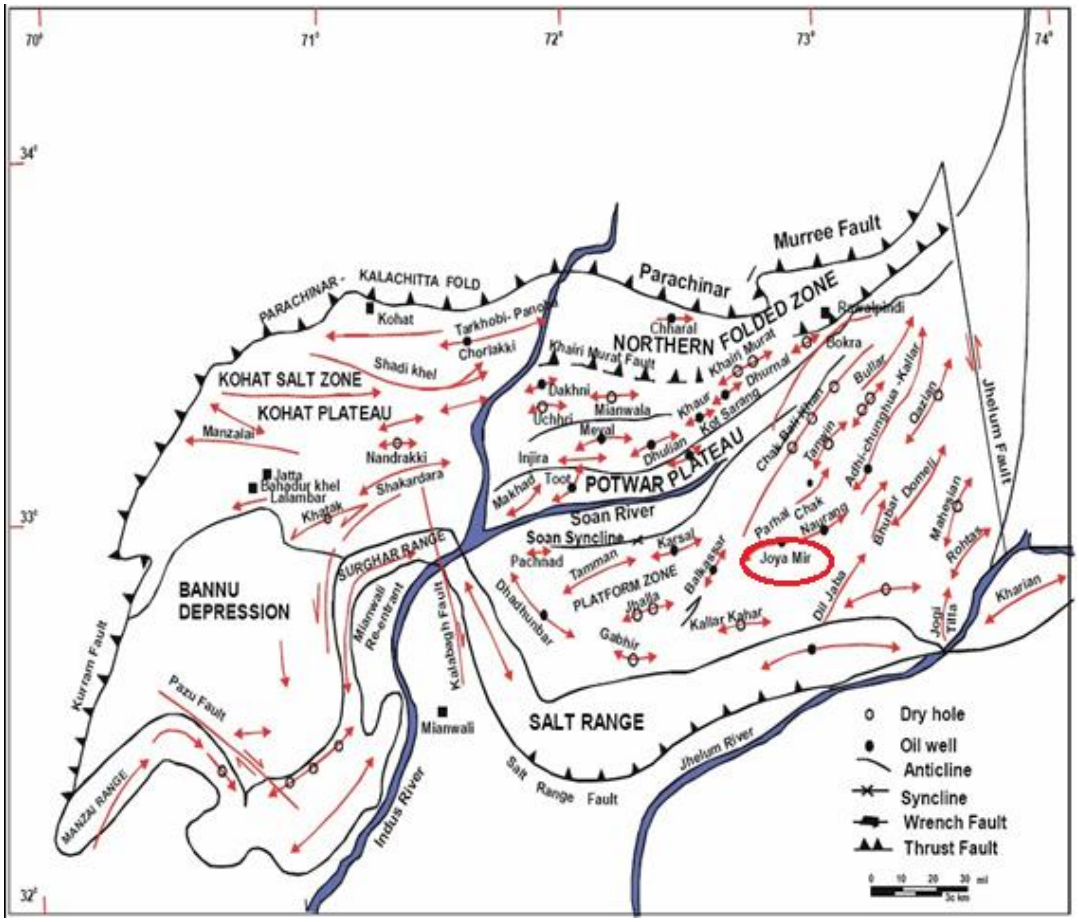

Fig.2.2 Tectonic divisions of Potwar Basin (Shami & Baig, 2003)

The Upper Indus Basin Joya Mair lies in the south-southeast of SRPFB (Salt Range-Potwar Foreland Basin). It was formed due to Tertiary Himalayan collision between Indian and Eurasian plate. It comprises of pre-Cambrian to recent rocks, which covers larger area of Indian plate. It consists of thick infra-Cambrian evaporates, thin Cambrian-Eocene calcareous-silici clastic sediments of Indian plate and relatively thick Miocene-Pliocene molasses deposits of Indus fore deep. The structural traps in the SRPFB are formed due to Himalayan folding and thrusting. Chak Naurang fault is passing through SRPFB. The Sakesar limestone and Chorgali are acting as the primary reservoirs while the Permian and Cambrian sandstone are acting as secondary reservoirs. The Eocene, Paleocene and Permian shale's are supposed to be the source and cap rocks.

2.3 Structural style of Potwar Plateau:

The structural style of the central eastern and western parts of Potwar Plateau shows a marked difference. In the central western parts of Potwar Plateau, the deformation appears to have occurred by south-verging thrusting, whereas in the eastern part the

deformation is mainly in northeast-southwest direction with tight and occasionally overturned anticlines separated by broad synclines. This difference may be related to lesser amount/thickness of salt in the lnfra-Cambrian in the eastern areas and very low dip of the basement (1°-1.5°) as compared to Central Potwar (2^0-3^0). In Central Potwar, structures are mainly fault bounded mostly by thrusts and back thrusts, while at some places, asymmetric anticlines are bound by a single fault. Based on the seismic interpretation, the structures in Potwar area may be divided into: Pop-up anticlines, Salt cored anticlines and Triangle zones (Moghal et al, 2003)

2.4 Local Structural Settings of Study Area

The Joya Mair oil field is located in the southeastern part of the Salt Range Potwar Foreland Basin (SRPFB). The study area shows a complicated structural configuration. The Joya Mair area is basically an anticline at the surface and plunges 10° southwest and 4° northeast (Shami et al., 2002). The fold axis of anticline trends northeast-southwest.

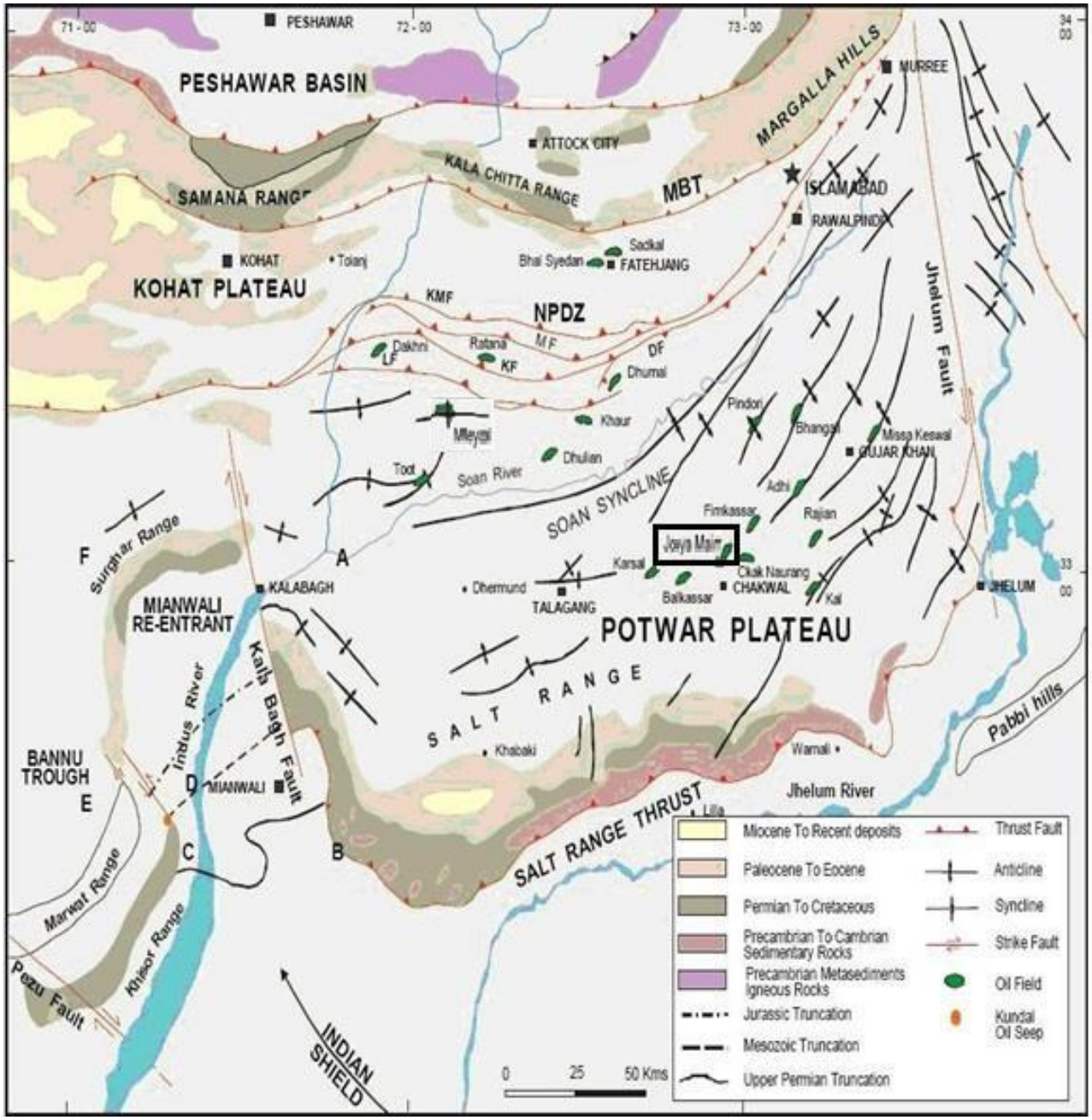

Fig.2.3 Geological and Structural Map of Potwar Plateau (Gee, 1989)

forming northeast-southwest trending Joya Mair Anticline. The formations which are exposed at the surface are Chinji and Nagri. The Chinji Formation is exposed at the core of the anticline and the Nagri Formation is exposed at the limbs and at places they are covered by alluvium. Seismic images of the Joya Mair oil field show that the Joya Mair structure is a triangle zone at the subsurface.

2.5 Joya Mair triangle zone :

The Joya Mair Triangle Zone is recognized on the basis of seismic survey which is a key structure for the exploration of hydrocarbons in foreland fold and thrust belts. The sedimentary rocks are deformed on the Precambrian evaporates of the Salt Range Formation in SRPFB. Borehole and seismic data shows that the Joya Mair structure is not a simple anticline. It is a triangle zone formed by the combination of thrust and backthrust, resulting in the triangle zone geometry at the subsurface and an open anticline at the surface. These thrust and back thrust phases in SRPFB are the result of northwest southeast Himalayan compression. (Aamir et al., 2006)

2.6 Generalized stratigraphy of the area:

Stratigraphy of the Joya Mair area is well established from the outcrop as well as from the wells drilled in the study area and the surrounding area. The stratigraphy of the Joya Mair area comprises of the Precambrian Salt Range Formation, Cambrian to Eocene Platform Sequence. In SRPFB the early to middle Cambrian Jehlum Group lies on the Salt Range Formation. The Jehlum Group includes Khewra Sandstone and Kussak Formation. The basin was uplifted during Ordovician to Carboniferous; therefore no sediments were deposited in SRPFB (Shami and Baig, 2002). The Cambrian Jehlum Group is disconformably overlain by the Permian Nilawahan Group. It includes Tobra Formation, Dandot Formation, Warchha Sandstone and Sardhai Formation. The Late Permian to Cretaceous rocks from west to east in the basin is eroded due to significant Pre-Paleocene tectonic uplift in SRPFB (Shami et al., 2002). The Early Paleocene marine transgression resulted in the deposition of Paleocene to Eocene carbonate-shale sequence. It includes the Lockhart Limestone**,** Patala, Sakesar and Chorgali formations. The Himalayan orogeny initiated the Eocene-Oligocene uplift and erosion in the SRPFB. The upper part of the stratigraphic section comprises of the Miocene to Pliocene non-marine Miocene molasse deposits include Murree, Kamlial, Chinji and Nagri formations.

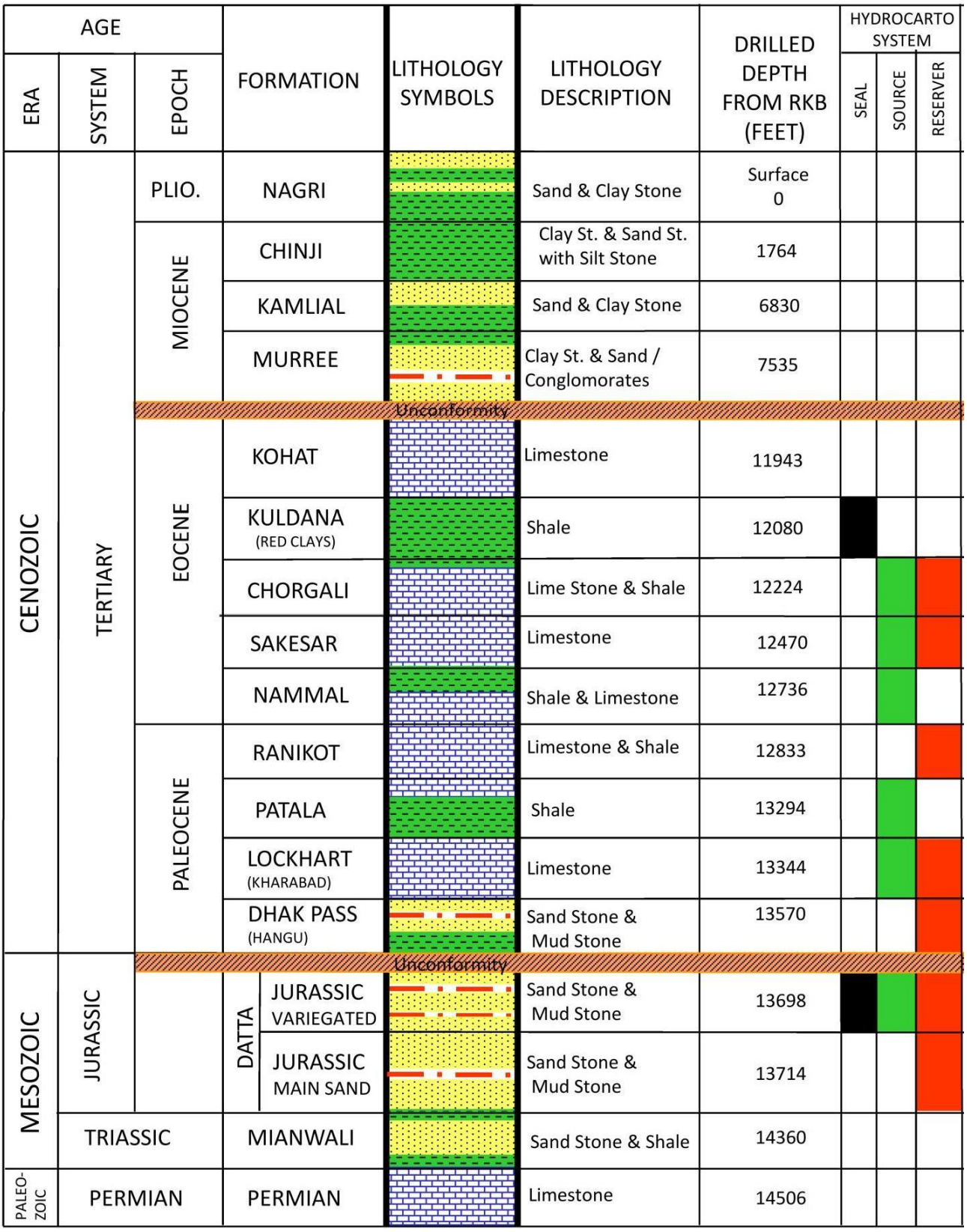

Figure 2.4: Generalized stratigraphic column of the area (Hasany and Saleem, 2001).

2.7 Petroleum Geology:

The Salt Range Potwar- Foreland Basin (SRPFB) belongs to the category of extra continental down warp basins, these accounts for 48% of the world known petroleum (Riva, 1983). It has several features suitable for hydrocarbon accumulation including continental margin, thin marine sedimentary sequence, potential source, reservoir and cap rocks. The thick overburden of 3047m of molasse deposits provides burial depth and optimum geothermal gradient for oil formation. The Salt Range Potwar- Foreland Basin (SRPFB) with an average geothermal gradient of 2 °C/100 m is producing oil from the depth of 2750-5200m (Shami and Baig, 2002). The presence of an optimal combination of source, reservoir and trap within the oil window resulted oil and gas accumulation in **Joya Mair**, Toot, Meyal and Dhulian oilfields (Kozary et al, 1968).

The Kohat-Potwar depression has several features that make it a favorable site for hydrocarbon accumulations. Located on a continental margin, the depression is filled with thick deposits of sedimentary rocks, including potential source reservoir and cap rock. It contains a thick overburden (about 3000 m) of fluvial sediments, which provide the burial depth and optimum geothermal gradient for seeps found in this area (Khan, et.al. 1986).

Simple and translated fault-propagation folds form important structural traps in fold and thrust belts. The most important traps in fault propagation folds are in the crests of major anticlines. These fault traps may be present along back-limb thrusts, between the imbricates in the forelimbs and in upturned beds in the footwall. Secondary traps may also be present within major thrust sheets, particularly at the leading edge of the thrust sheet and above footwall ramps (Mitra, 1990).

2.8 Reservoir Rocks of Potwar Basin

Although the effective reservoir at Joya Mair oil field lies within the Sakesar and Chorgali formations, the Nammal and formations are also worth mentioning in this area because these formations (Nammal, Sakesar, Chorgali) are part of the same depositional

sequence (Vail et al., 1977). The Nammal, Sakesar, Chorgali Sequence were deposited on a ramp which fits the classic models for Tertiary low latitude carbonate ramps

(Buxton and Pedley, 1989). These are characterized by slope gradients of less than degree and extend 10 to 100 of kilometers along strike (Buxton and Pedley, 1989). Hence Paleozoic- Tertiary dominantly marine sedimentary rocks form petroleum systems in Potwar basin and are exposed in Salt Range along the frontal thrust and the fractured carbonates of Sakesar and Chorgali formations are the major producing reservoirs in the study area.

2.8.1 Chorgali Formation

The Chorgali Formation is named following Chorgali Pass that transects the Khair-e-Murat ridge near the village, Pind Fateh. The formation consists of massive dolostones, marls, nodular, extremely fissile varicolored shales, and evaporite collapse breccias. It is 80 to 90 m thick (Jurgan and Abbas, 1991) and is early middle Eocene in age (Gingerich, 2004). There is very slight primary porosity and appears as vugs in certain layers and the process of dolomitization has produced porosities up to 25 % (Malik et al., 1988).

2.8.2 Sakesar Formation

The Sakesar formation is named following Sakesar town in the Salt Range where it is well exposed. It is major formation, acting as reservoir producing both Oil and Gas in Fimkassar area. It is a fractured reservoir, having negligible porosity (matrix). It is about 70 to 300 m thick and is early to middle Eocene in age (Bender and Raza, 1995). The production from Sakesar commenced in 1980, and this formation is encountered in all the wells, used in research. Fimkassar-01, drilled at the apex, encountered Eocene more than 100 m shallower compared to Turkwal-01 and Turkwal Deep-01, while in Turkwal Deep- X2, it is more than 1,000 m shallower.

2.9 Source rock:

The grey shale's of Mianwali, Datta, and Patala formations are potential source rocks in SRPFB. The oil shale's of Eocambrian Salt Range formation includes 27% to 36% TOC in isolated packets of shale's, and are considered as source rocks in SRPFB.

2.10 Reservoir rocks:

The Cambrian, Permian, Jurassic, Paleocene and Eocene reservoirs are producing oil in SRPFB. The fractured carbonates of Sakesar and Chorgali formations are the major

producing reservoirs in Joy Mair. The Sakesar limestone is light yellow grey, massive and partly dolomitize and locally contains chart concretions. The Chorgali formation is creamy yellow to yellow grey, silty, partly dolomitic and thin bedded limestone. The Chorgali formation was deposited under supratidal to intratidal conditions where sabkha condition dominated. Interskeletal and intraskeletal porosity is mainly common in Sakesar and Chorgali formation. The pores spaces at places are filled by calcite cement. Primary porosity is less than 1% in Sakesar and Chorgali formation. Most of their porosities were developed by dolomitization, leaching of fossils and anhydrite moulds. The fracture porosity is relatively higher in wells of northwestern Potwar because the rocks deformed several time during Himalayan orogeny. (Houston et al., 1996)

2.11 Traps:

Traps have been developed due to thin-skinned tectonics, which has produced faulted anticlines, pop-up and positive flower structures above Pre-Cambrian salt. The clays and shale's of the Murree Formation provide efficient vertical and lateral seal to Eocene reservoirs wherever it is in contact.

2.12 Cap rock:

In Potwar area most of the structures are anticlinal and thrusted anticlinal due to Himalayan orogeny. The Kuldana formation acts as a cap for the reservoirs of Sakesar. and Chorgali formations in SRPFB. The clays and shale's of Murree formation also provide vertical and lateral seal to Eocene Reservoirs in SRPFB wherever it is in contact.

2.13 Migration and Accumulation:

The Paleocene reservoirs show favorable properties for migration and accumulation of oil in SRPFB. The Eocene carbonates of Sakesar and Chorgali show common intergranular, intra skeletal dissolution and moldic porosity. The limestone is deposited in supratidal to intratidal environments, indicating very low primary porosity, which averages from 1-3% as obtained through the core analysis of Joya Mair, Dhulian and Meyal oilfields.

The dominant secondary porosity in these carbonates is the fracture porosity. The secondary porosity need to be worked out for exploration under these conditions. The

fracture trend study indicates that the migration of oil within the structure occurred upward and laterals in northeast-southwest and northwest-southeast directions.

The oil migrated and accumulated in the hanging wall anticlines of the southeastern and northwestern flanks of the triangle zone. The oil is trapped in the hanging wall anticlines because the clays of the Murree formation lie in the footwall and above the Paleocene reservoir. The accumulation of oil in the hanging wall anticline of the southeastern flank is proven by the drilled oil wells in the Joya Mair oilfield. The similar hanging wall anticline occurs along the northwestern flank of the triangle zone.

CHAPTER 03 SEISMIC DATA INTERPRETATION

3.1 Introduction:

The Seismic interpretation is the process of determining information about the subsurface of the earth from seismic data. It may determine general information about an area, locate prospects for drilling exploratory wells, or guide development of an already-discovered Field (Coffeen, 1986). Conventional seismic interpretation implies picking and tracking laterally consistent seismic reflectors for the purpose of mapping geologic structures, stratigraphy and reservoir architecture. The ultimate goal is to detect hydrocarbon accumulations delineate their extent and calculate their volumes. Conventional seismic interpretation is an art that requires skill and thorough experience in geology and geophysics. To meet the challenges of exploring ever increasingly complex targets, there have been tremendous advancements in data acquisition equipment, computer hardware and seismic processing algorithms in the last three decades. The seismic method has thus, evolved into a computationally complex science. The computer-based working (Processing & Interpretation) is more accurate, precise, efficient and satisfactory which provides more time for further analysis of data. This whole work is carried out using by the computer software products, which is SMT Kingdom suit.

3.2 Structural Interpretation:

Seismic data interpretation is mainly done on the basis of available information and stratigraphy of the area. Seismic is correlated with the formation tops penetrated in the wells using well tops if available. In this study, seismic interpretation is done by picking horizons in Kingdom suit and reflector is continued in all other seismic lines. Major faults are picked on the dip lines and their parts are correlated across the strike lines to map the structures throughout the area. Misties are major concern during interpretation, which is resolved by using of bulk shift of different time. Two-way time (TWT) maps are generated using fault polygons in order to describe the structural inclination at different levels. The study area is in compressional regime, pop up and snaked head structures are

present in the area. The horizons which are marked on seismic section show thrust and

reverse faulting. Faults are oriented in the northeast-southwest (NE-SW) direction Comparing all the maps it is obvious that pop-up and snaked head structures are present in the study area. Navigations and SEG-Y of given six seismic lines of Joya Mair area are loaded in software (Kingdom Suit) and following procedure is adopted as shown fig.3.1

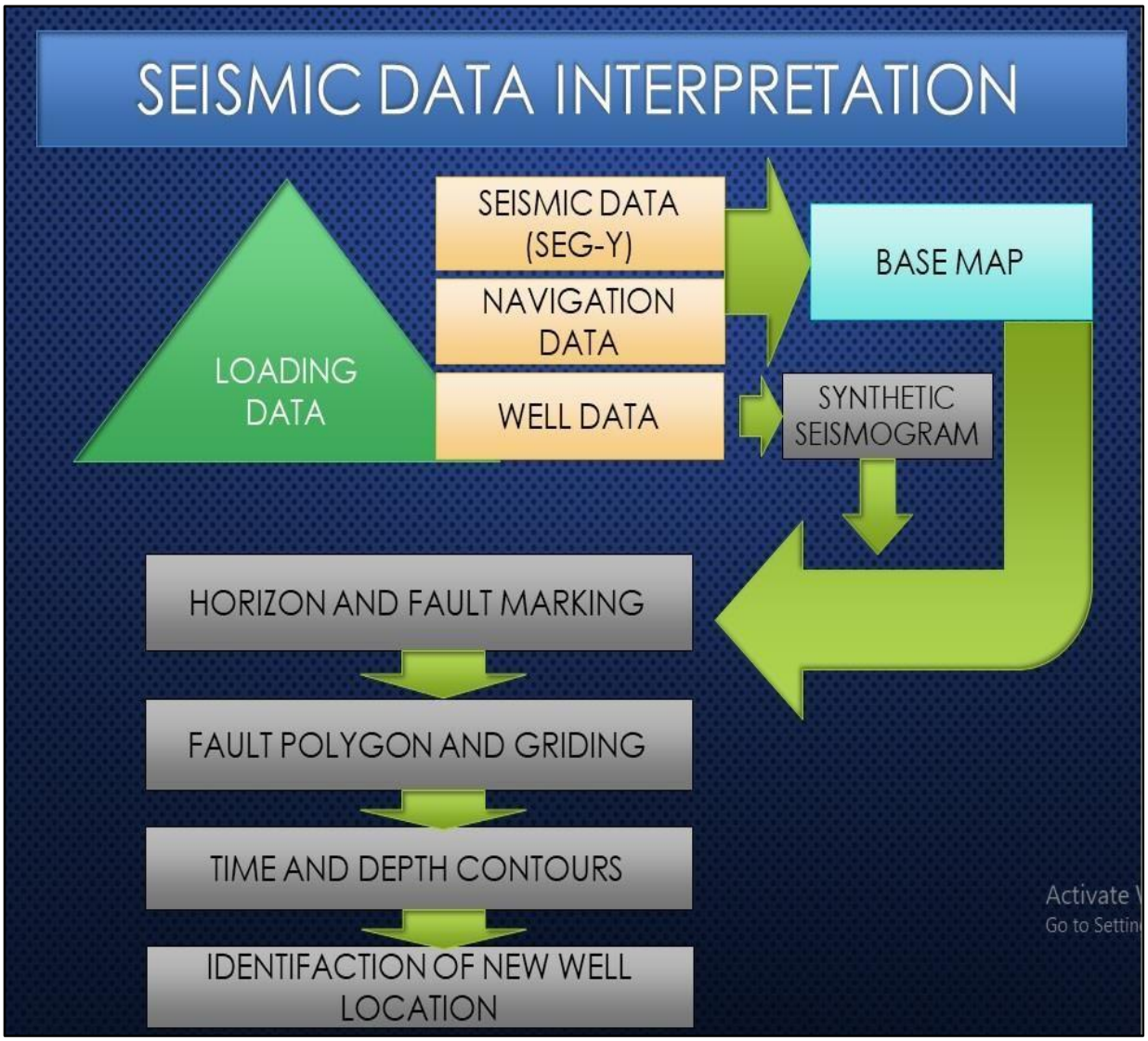

Fig 3.1. Interpretation workflow.

3.3 Seismic section:

Seismic section is the outcome of the seismic reflection survey. The seismic section shows the high values of traces in vertical line which are called recorded peaks in the cross section. Most importantly it points out some the features of a geologic cross-section. These high value traces in seismic section is filled in with black shows the

wiggle-variable area. The seismic section display or plot the data of the seismic line. The vertical scale in the seismic section displays the arrival time (Two way travel time).Seismic section plots or displays seismic data along a line. The vertical scale is usually arrival time but sometimes depth and the Horizontal axis shows the shot points and CDP.

3.4 Seismic horizon:

The reflection that can be traced across a seismic section is called a seismic horizon. In seismic sections the basement show no good continues reflection and has very short disordered and discontinues reflection. The geology of the area it reveals that it has salt in its basement. The horizon named Chorgali Formation is marked on the basis that it is producing reservoir in the area and has excellent visibility and good continuity of reflection so we can trace it well over the whole seismic lines. So this horizon can be easily recognized in the seismic section. Hence two-way travel time for the Chorgali Formation was taken from the Time to depth graph as shown in Figure 3.3.

The pink line marks the Rawalpindi Group the green line mark Chorgali Formation reflector the orange line mark Sakesar Formation and the blue line mark the permin reflector. Whereas the yellow lines mark the faults observed in the seismic lines. The Minwal X-01 is drilled in the seismic line 93-MN-08 at shot point 200, to a TWT 1.3 sec.

So, the seismic section shows that this area is characterized by thrust faulting (oppositely dipped). These thrust faults have shaped the strata a thrust related monocline on the hanging walls while a drag synclinal structure on the foot wall as shown in Figures 3.3,fig 3.4 ,fig 3.5 ,fig 3.6 ,fig 3.7 ,fig 3.9

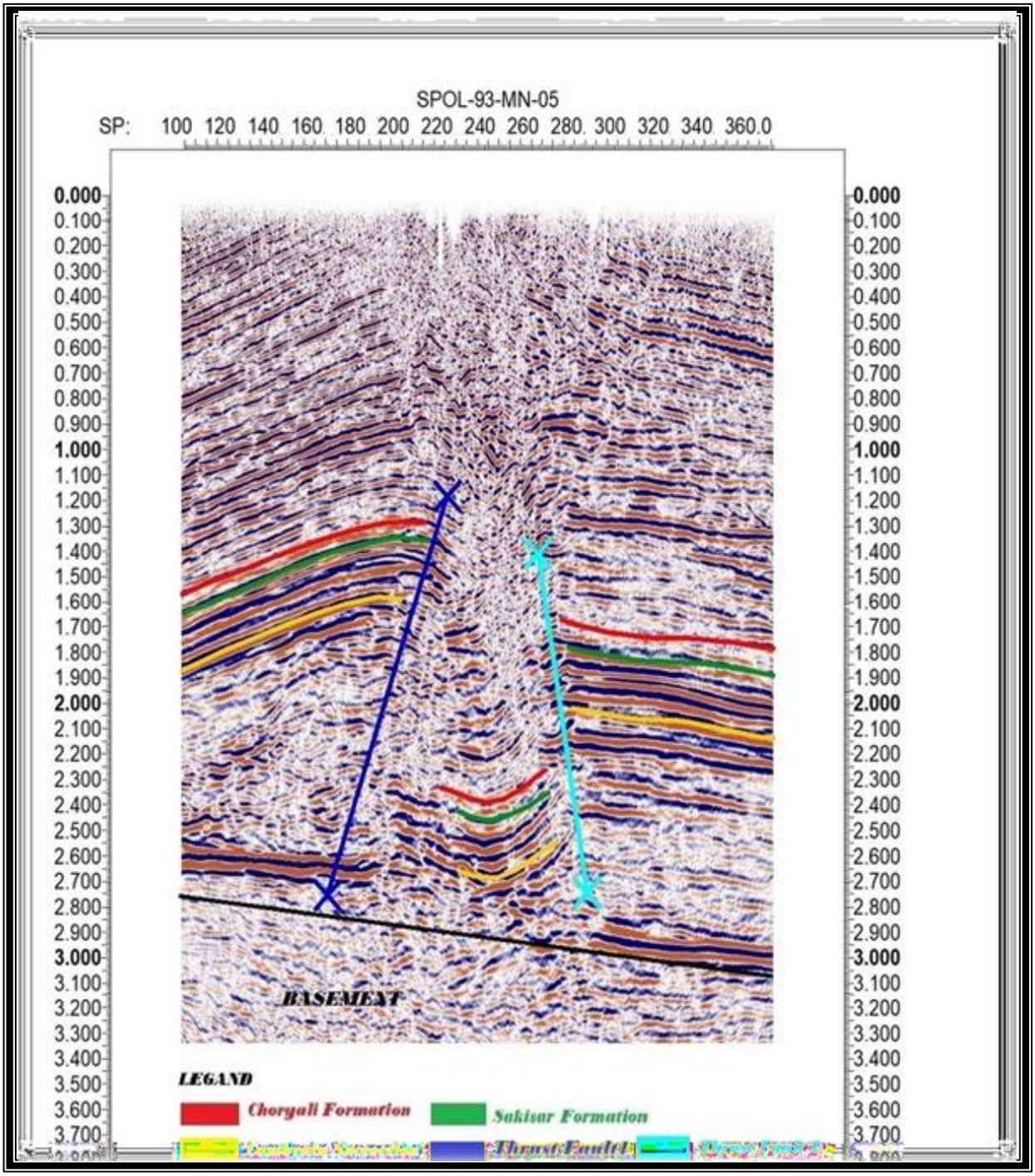

Fig 3.3 Interpreted seismic line SPOL-93-MN-05

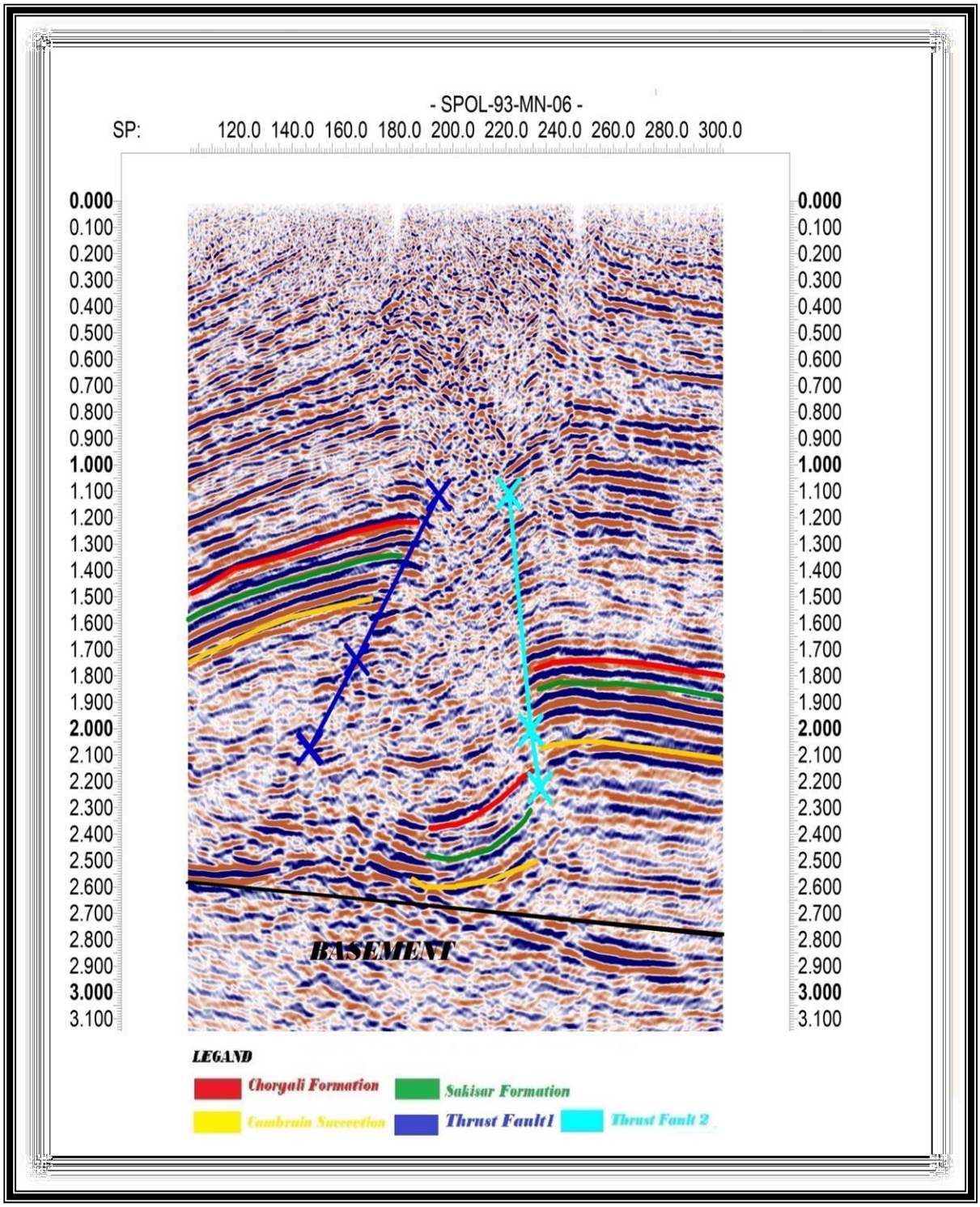

Fig 3.4 Interpreted seismic line SPOL-93-MN-06

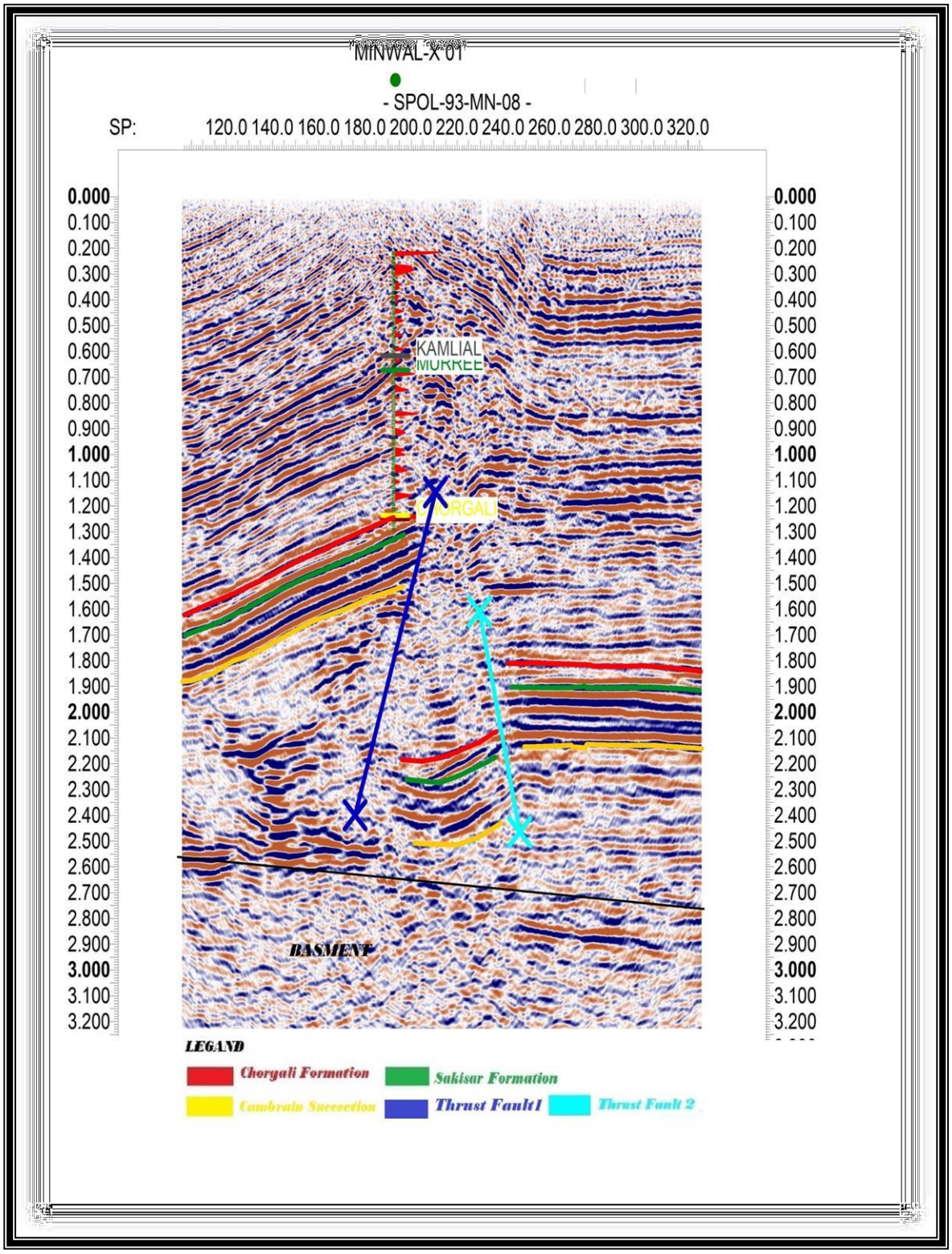

Fig 3.5 Interpreted seismic line SPOL-93-MN-08

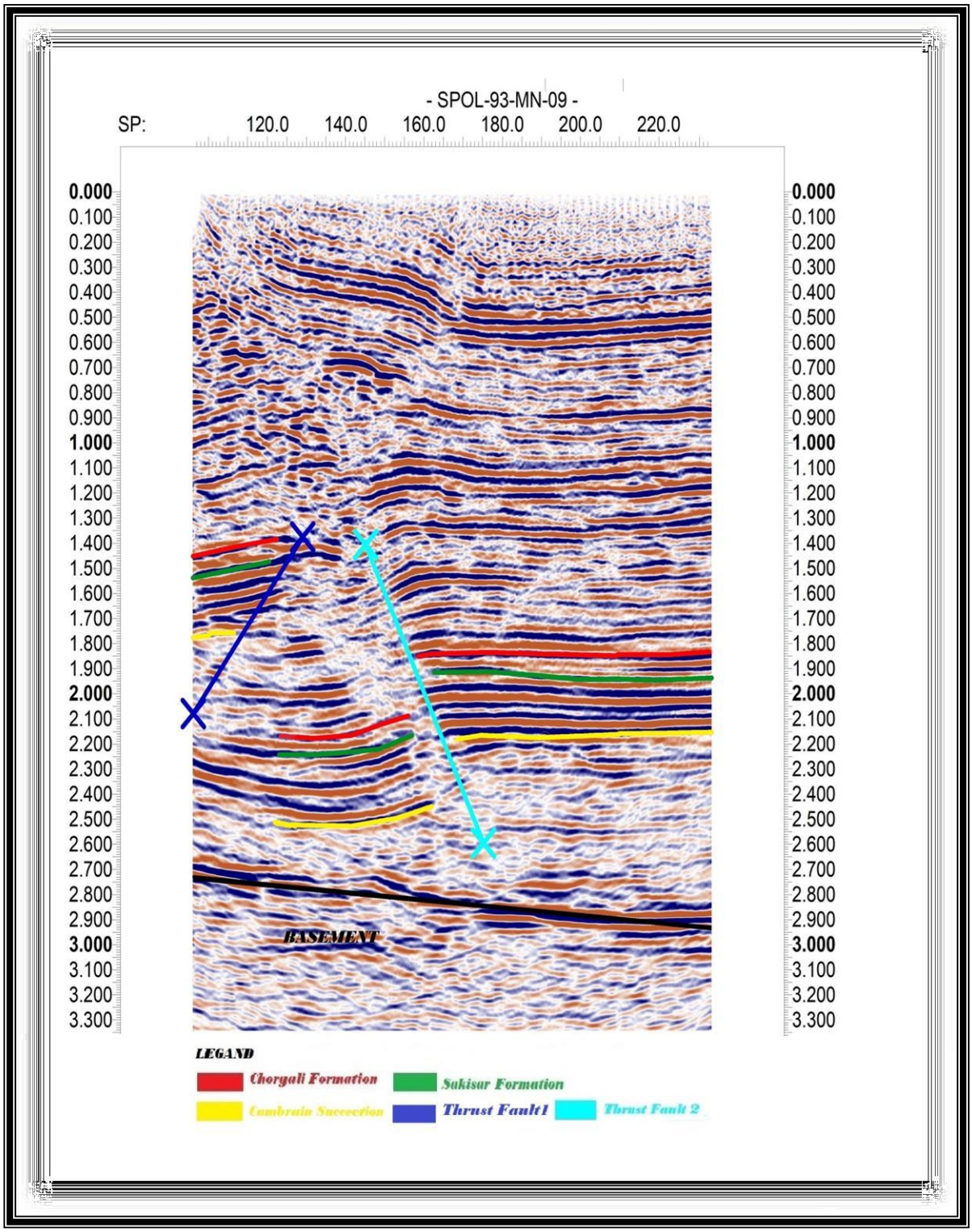

Fig 3.6 Interpreted seismic line SPOL-93-MN-09

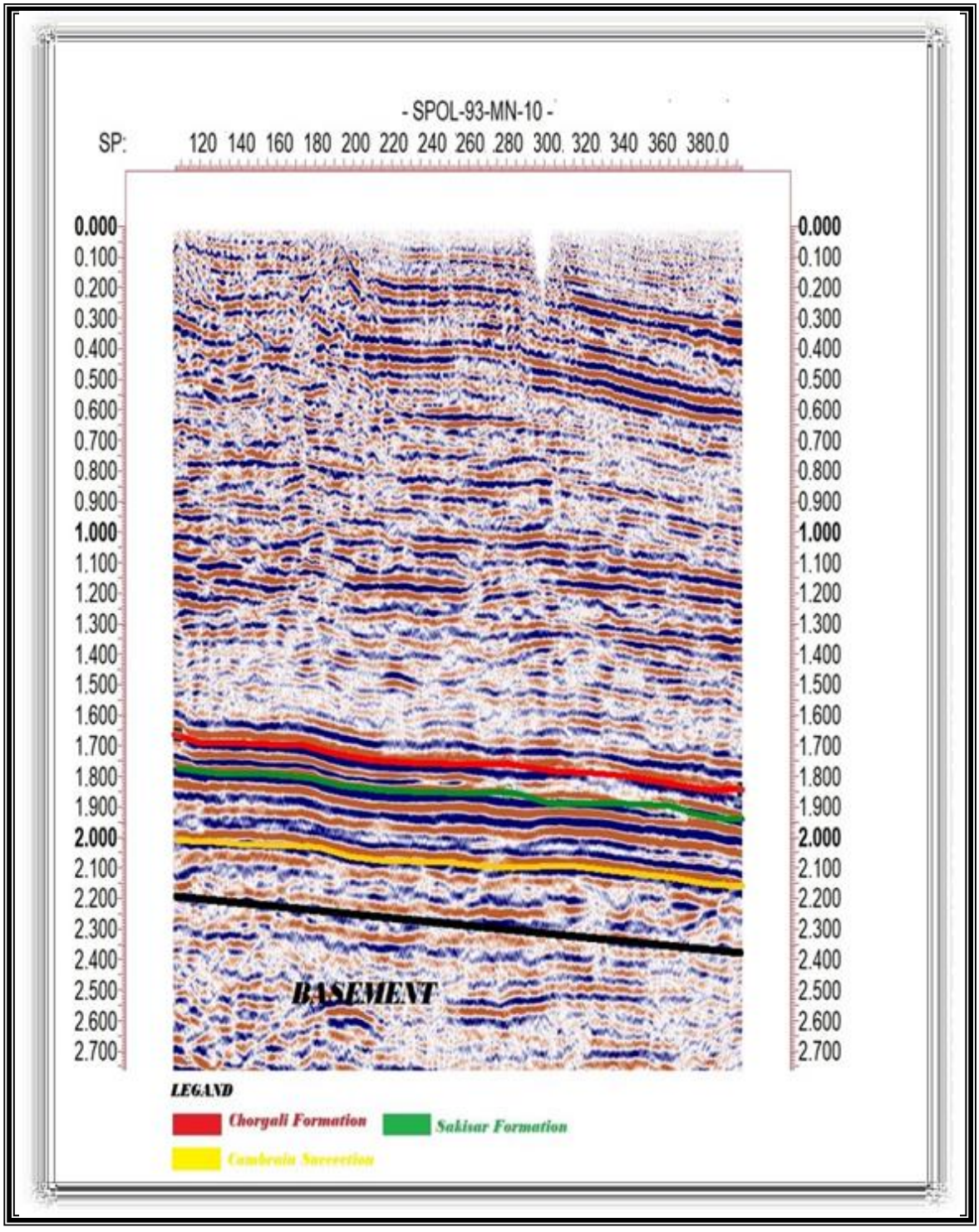

Fig 3.7 Interpreted seismic line SPOL-93-MN-10

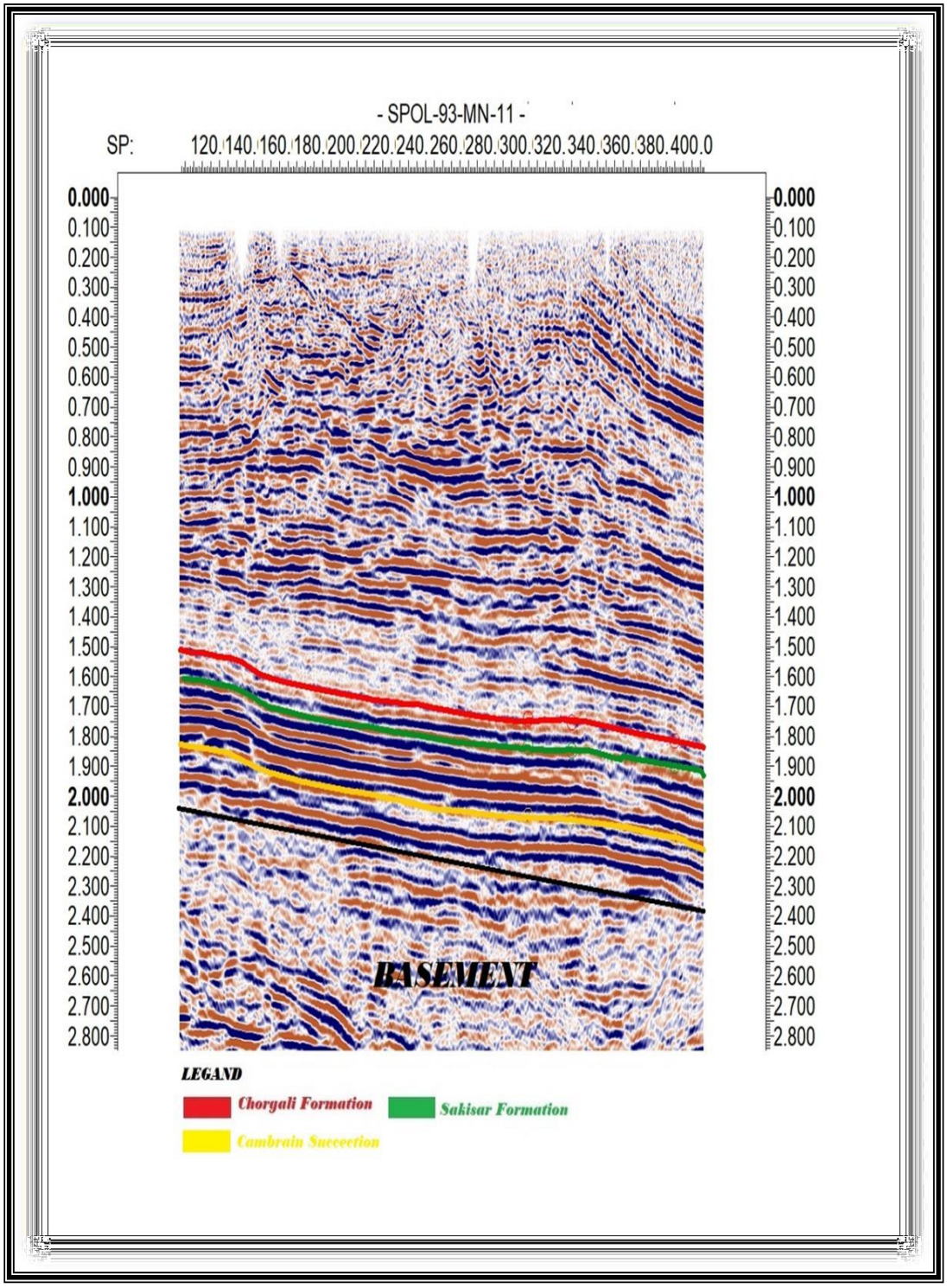

Fig 3.8 Interpreted seismic line SPOL-93-MN-11

3.5 Fault Polygon on structure:

I construct the fault polygon at Chorgali and Sakesar because the Chorgali and Sakesar acting as reservoir in my study area. The fault polygon on both these level as show the fig

3.5.1 Fault Polygons of Chorgali:

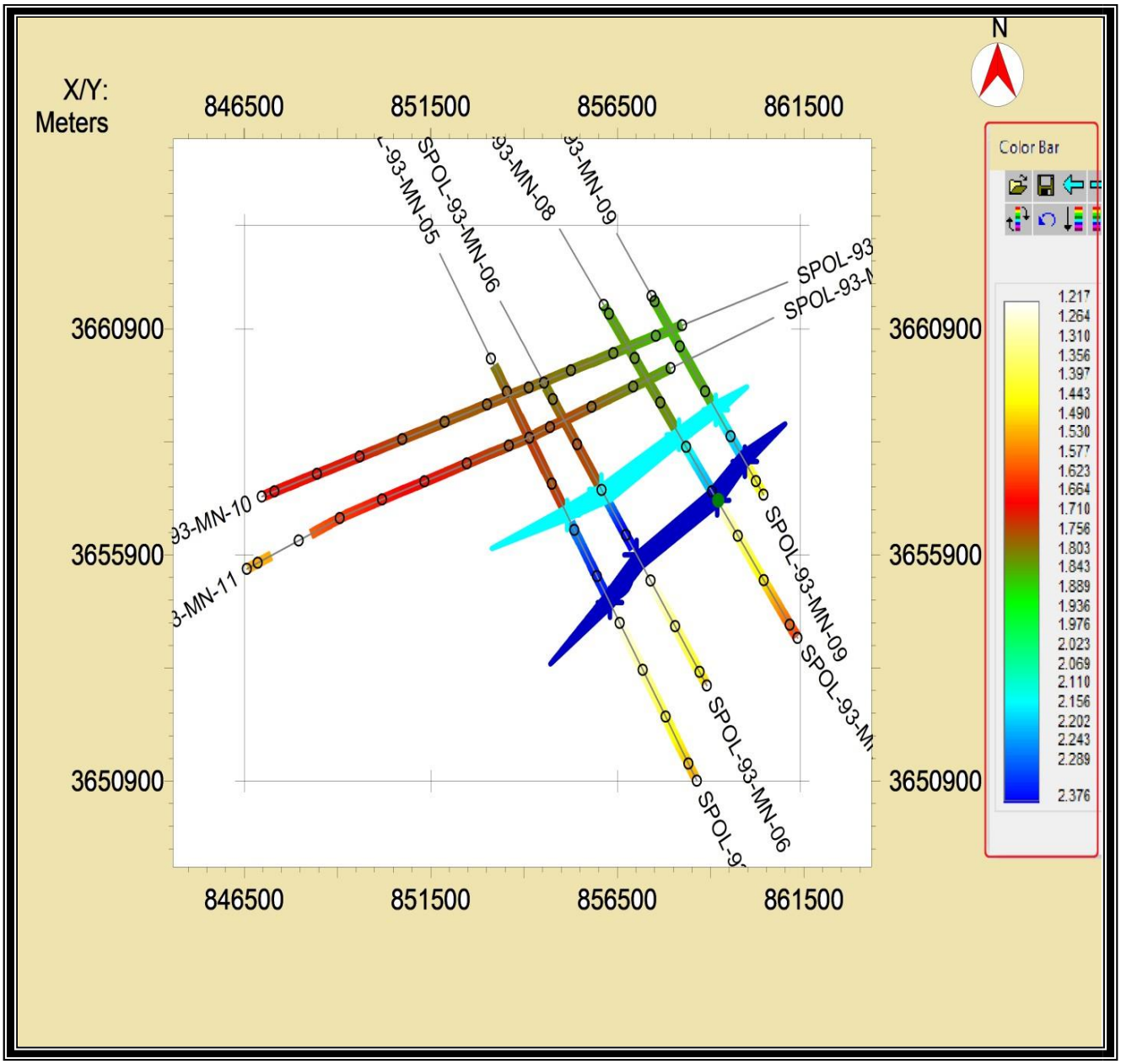

Fig3.9 Fault polygon at Chorgali

3.5.2 Fault Polygons of the Sakesar:

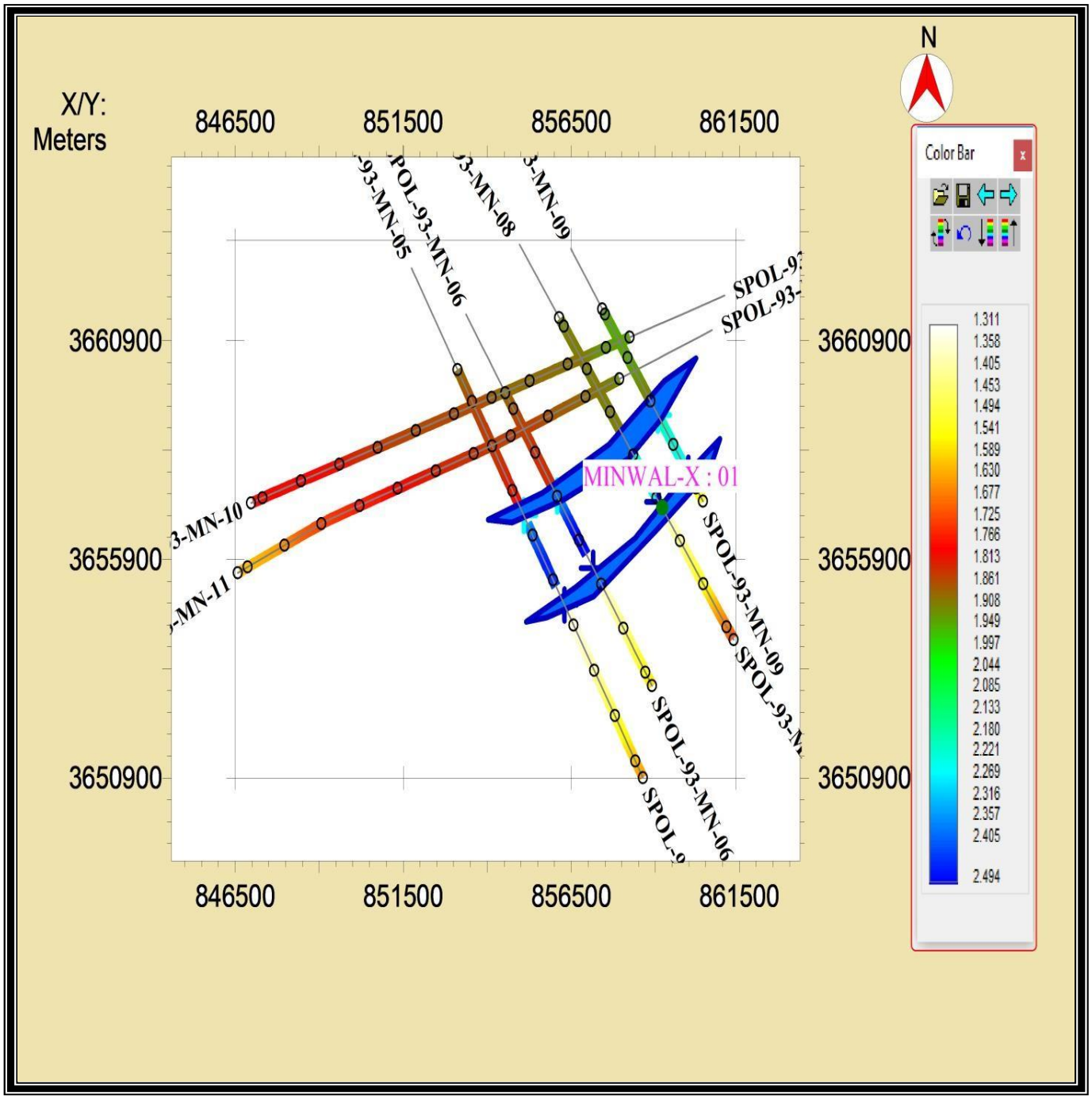

Fig3.10 Fault polygon at Sakesar

3.6 Contour maps:

A line that connects the line of equal values is called a contour line. Such maps show us steepness of slopes, elevation top of the subsurface of the sedimentary rock layer and also the two-way travel time of the horizon in millisecond (Norman, 2001).

- Time Contouring

- Depth Contouring

3.6.1 Time contouring:

In time contouring we discuss the study area of Joya mair oilfield (Potwar upper Indus basin) which contains Rawalpindi Group, Chorgali Formation, Sakesar Formation, Permian succession through:

- Time contour
- Time surface
- Time surface with contouring
- Time surface with contouring and dipping direction
- Time surface with contouring and hydrocarbon flow direction

Time was taken from the seismic section. The next step was the generating the time contour map. As the time was in milliseconds so it is converted into seconds and then plotted into the base map and is contoured and then its time surfaces were generated the time contour map and time surfaces of Rawalpindi group and Chorgali is discussed.

3.6.2 Depth contouring:

The depth contour map marks the depth of structure. The depth contour map in the subsurface mainly shows the faults, anticline and folds.

So, after marking the time contour map the depth contour map is being generated by using the following formula.

$$S=V*T/2 \ldots\ldots \text{(i)}$$

Hence, we have the time and depth of the given formation (Rawalpindi group, Chorgali Formation, and Sakesar). 1st we find velocity of each formation by using the formula.

$$V=2*S/T$$

Then put it in the equation (i) to calculate the depth of each formation then using it for

depth contour mapping. Depth contouring of the area can be discussed by

- Depth contouring
- Depth surface
- Depth surface with contouring
- Depth surface with contouring and dipping direction
- Depth surface with contouring and Hydrocarbon flow direction

3.7 Chorgali Formation time and depth contouring:

The depth contour maps of Chorgali Formati0were generated by joining the points of equal depth. These depth values have assigned a color bar which can be used as a guide for interpretation. On the color bar orange color shows the shallowest point which also give us information about the probable well location (probable well position#1,probable well position#2 and probable well position#3) while the purple color represents deepest point .The time contour map of Chorgali Formation was generated by joining the points of equal times. These time values have assigned a color bar which can be used as a guide for interpretation. On the color bar orange color shows the shallowest point while the purple color represents deepest point as shown in figures as shown

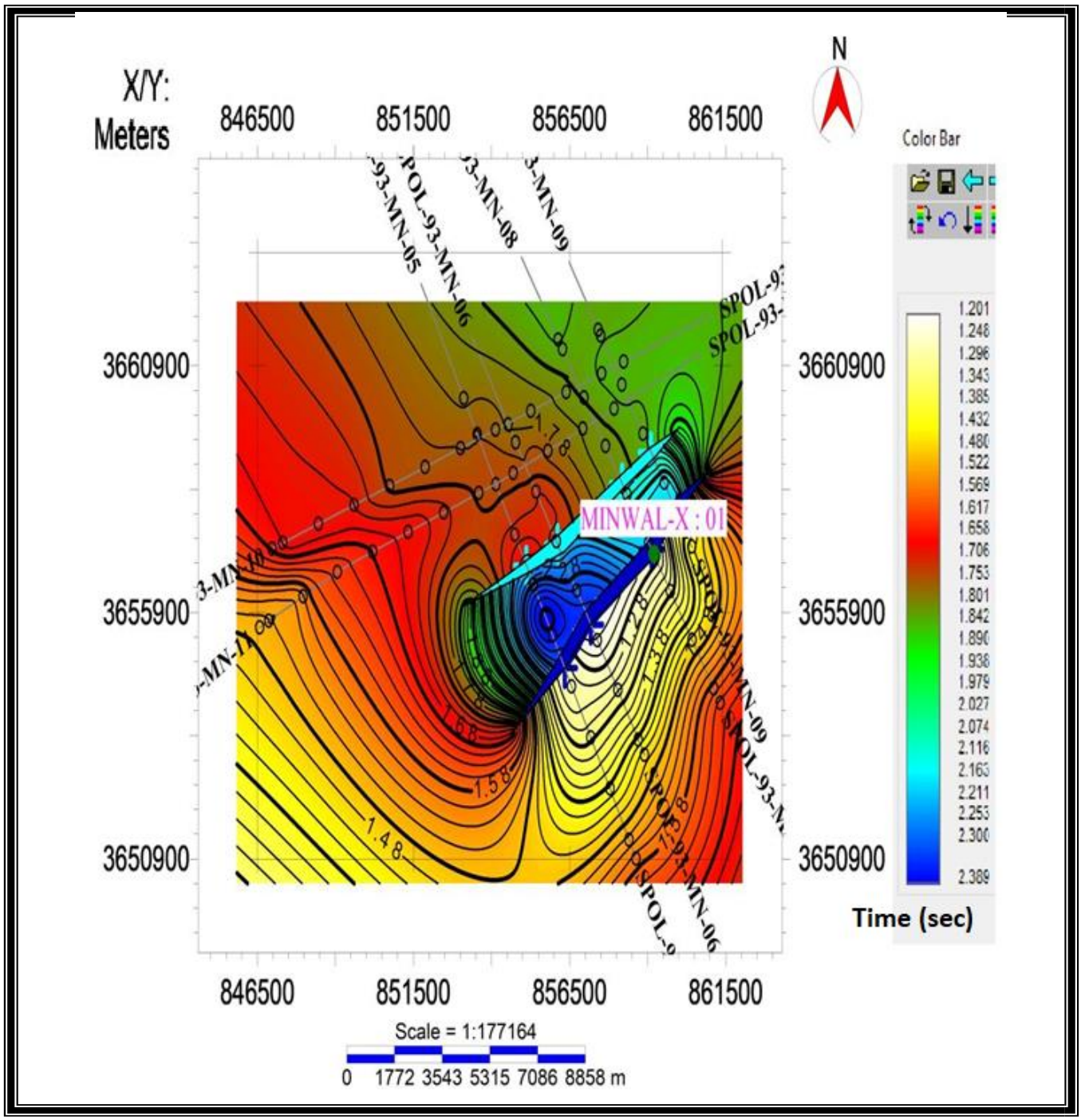

Fig 3.11. Time contour map of Chorgali formation

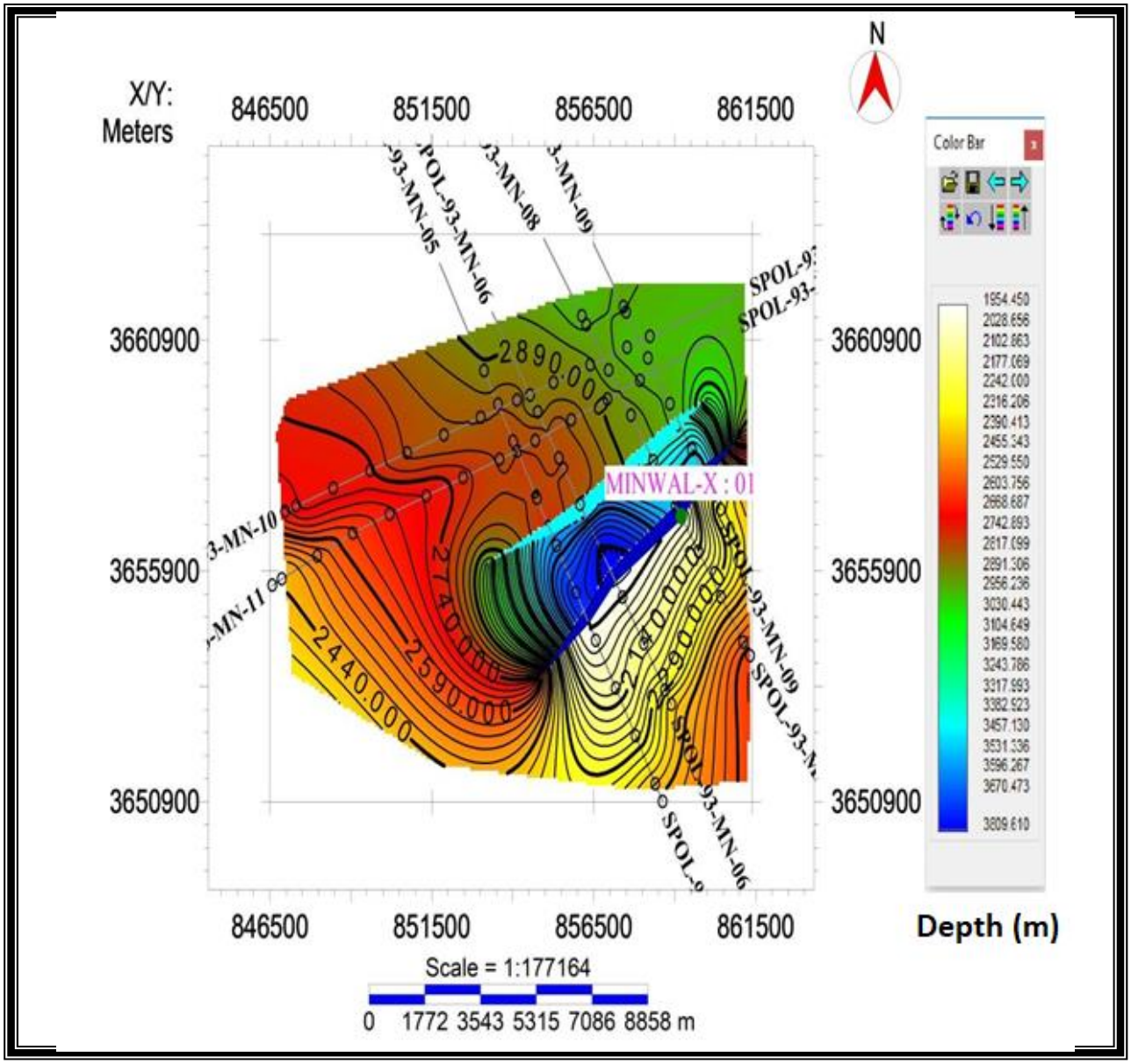

Fig 3.12 Chorgali formation depth contouring:

3.8 3D View of time contour map of Chorgali:

The contours show oppositely dipping having a thrust monoclonal structure on their hanging walls and thus forming triangle zone in the subsurface. After this time surface were generated which visualize our interpretation in 3D views These time surfaces were

also displaced with the dipping direction of the strata, which indicate the dipping of strata at each and every point on these time surfaces probable hydrocarbon flow were marked which show us the points of Hydrocarbon accumulation.

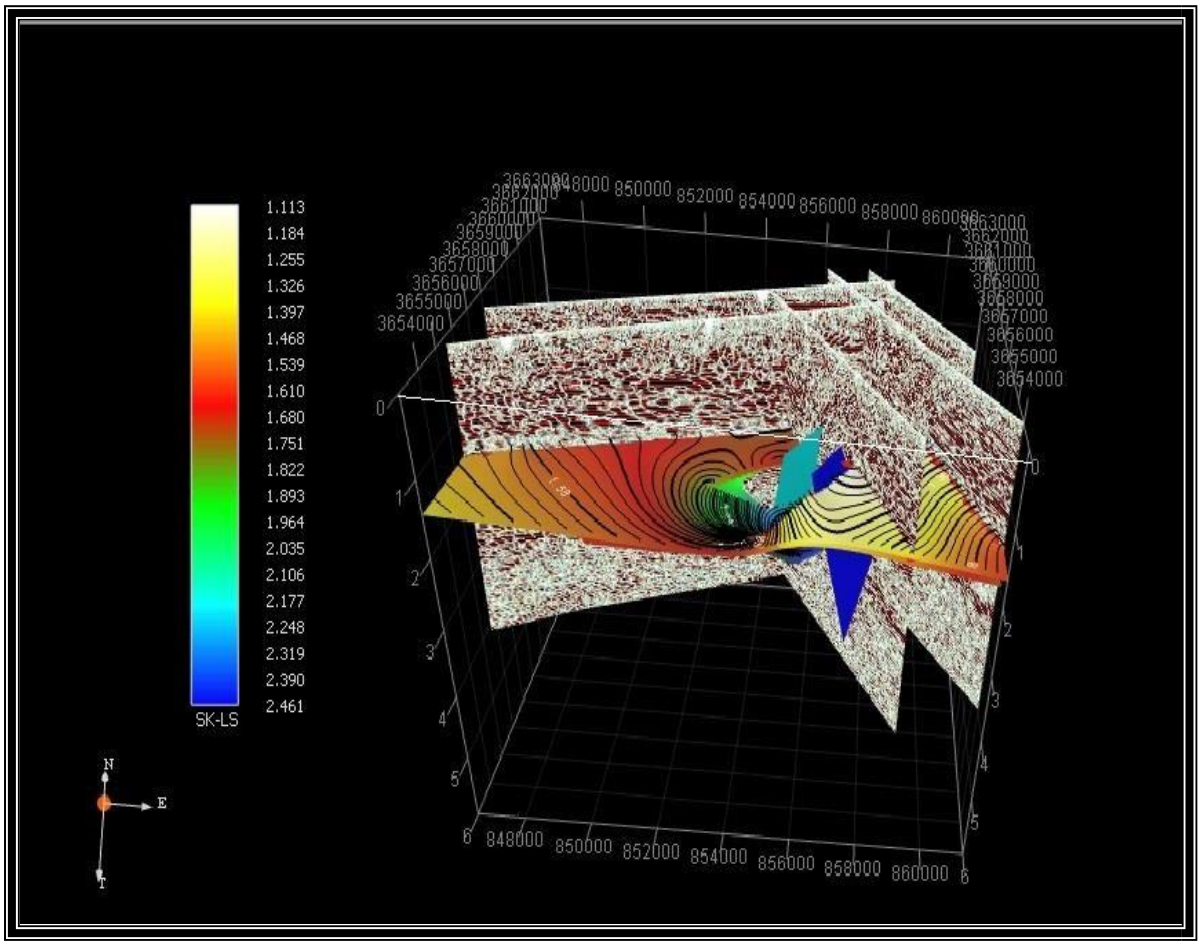

3D View of time contour map of Chorgali:

3.9 Sakesar Formation time and depth contouring:

The time contour map of Sakesar was generated by joining the points of equal times. These time values have assigned a color bar which can be used as a guide for interpretation. On the color bar orange color shows the shallowest point while the purple color represents deepest point as shown in figure

The depth contour map of Chorgali Sakesar was generated by joining the points of equal depth. These depth values have assigned a color bar which can be used as a guide for interpretation. On the color bar orange color shows the shallowest point which also give us information about the probable well location (probable well position#1, probable well position#2 and probable well position#3) while the purple color represents deepest point as shown

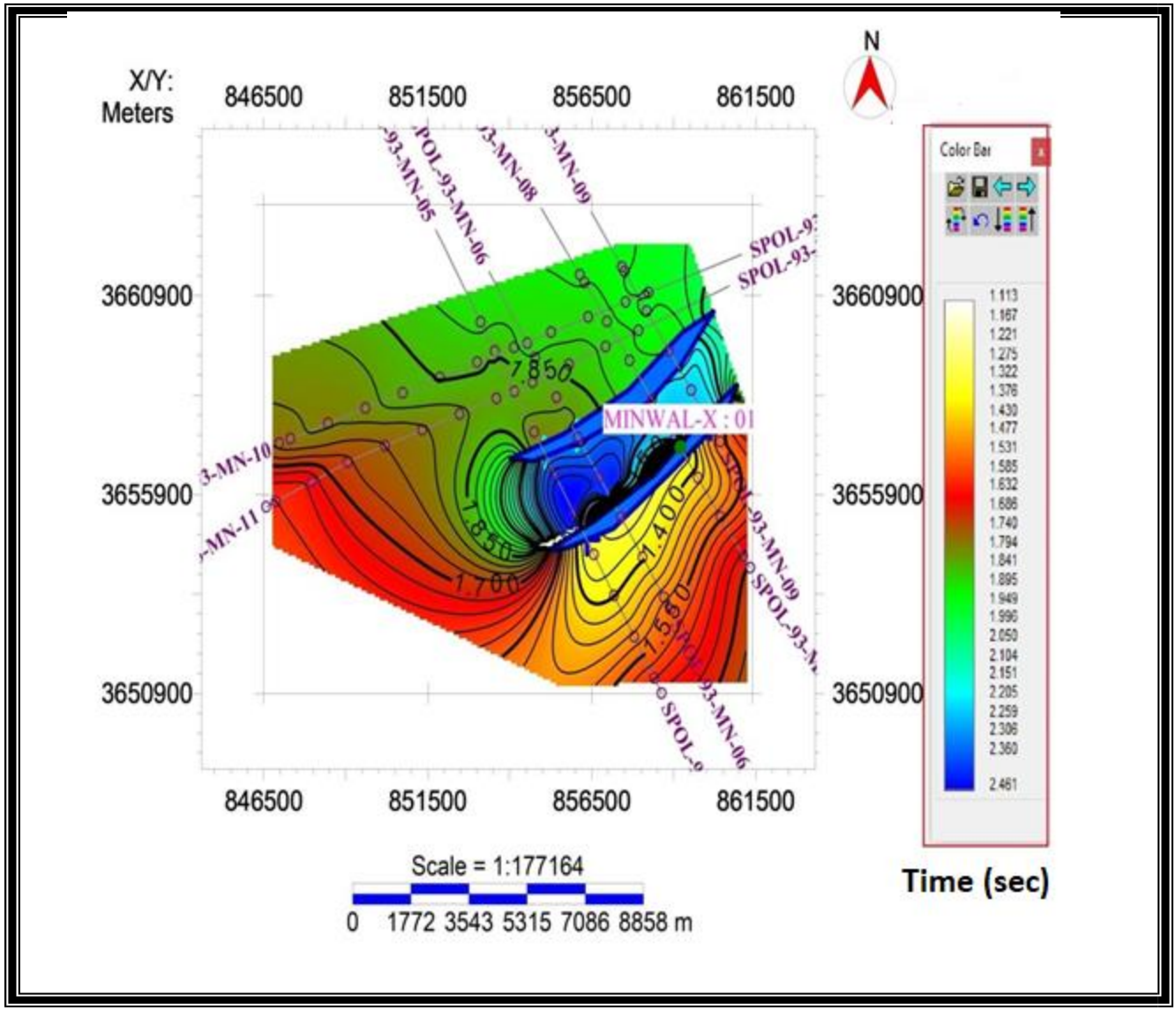

Fig 3.14 Sakasr Formation Time contouring

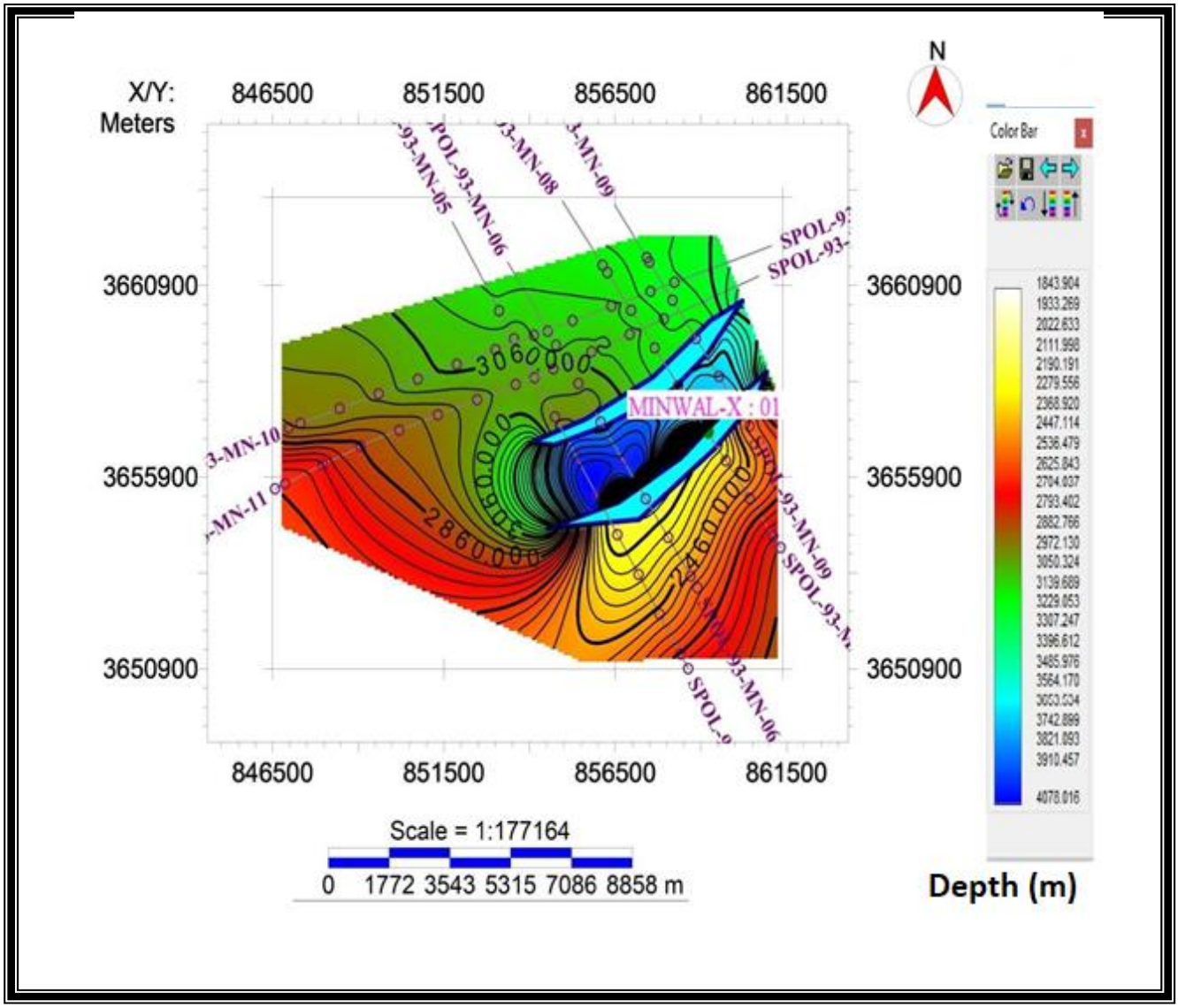

Fig3.15 Sakesar Formation Depth contouring

3.10 3D View of time contour map of Sakesar:

The contours show oppositely dipping having a thrust monoclonal structure on their hanging walls and thus forming triangle zone in the subsurface. After this time surface were generated which visualize our interpretation in 3D view These time surfaces were also displaced with the dipping direction of the strata, which indicate the dipping of strata at each and every point

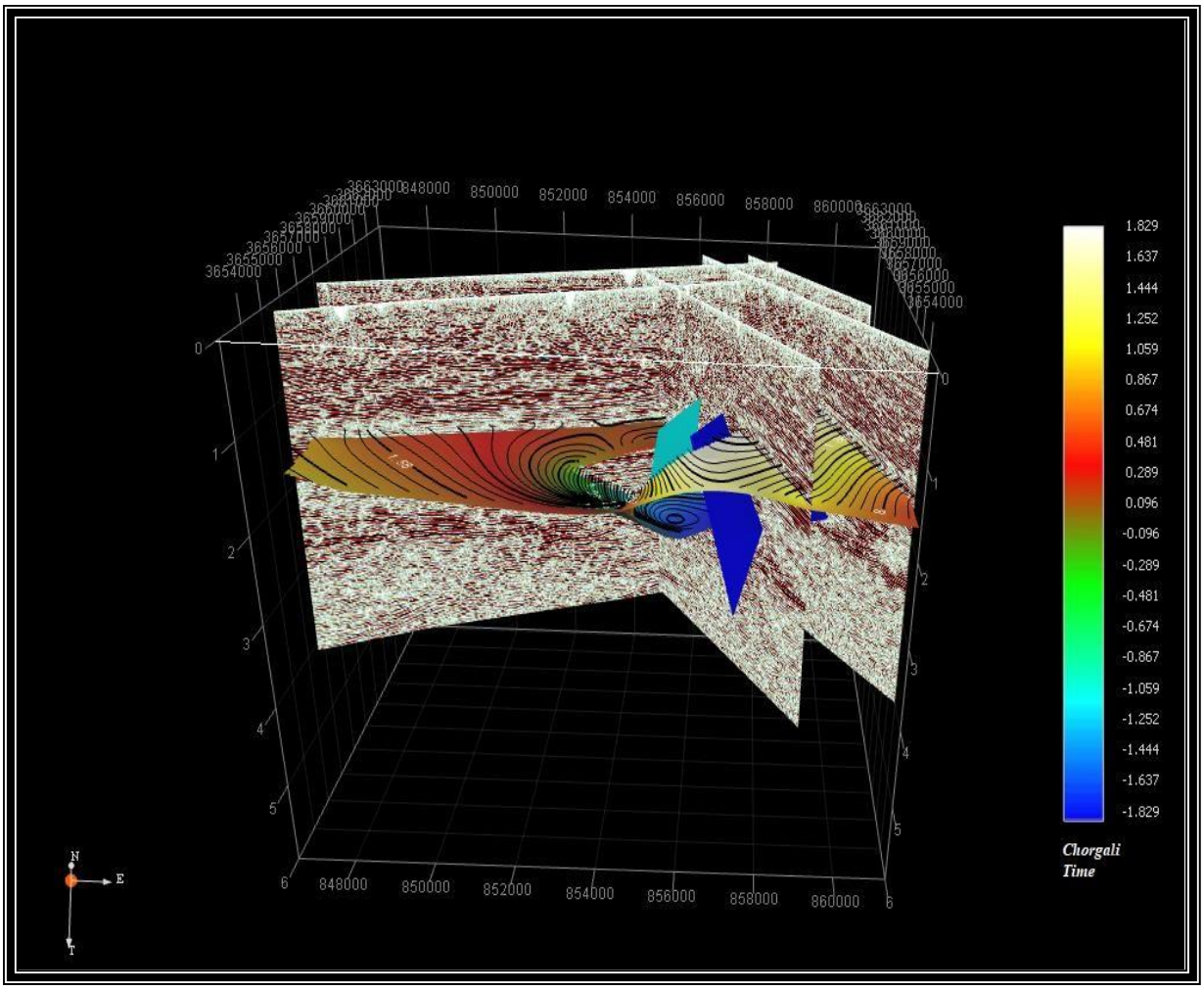

Fig.3.16 3D View of time contour map of Sakesar:

3.11 1-D Forward Modeling:

In Seismic surveys the ground motion over a short interval of time, following a seismic Source, is measured. The graphical plot of the output of a single detector is called "Seismogram". An artificial seismic reflection record prepared from velocity log data by convolving the reflectivity function derived from digitized acoustic and density logs with the wavelet derived from seismic data is termed as "Synthetic Seismogram". Synthetic seismogram is an artificial model of the Earth that is contracted to mark the different geological horizon on the seismic section. It is direct one-dimensional model of acoustic energy traveling through different layers of Earth.

The synthetic seismogram can be of great value to the interpreter and it is best presented by splicing it to an interpreted seismic section through the well location

(Peterson et al., 1955; Baranov and Kunetz, 1960). Synthetic seismogram of Meyal-08 well is generated using Wavelets software (Khan et al., 2006). In this procedure the petrophysical logs; Sonic (DT) and Bulk Density (RHOB), which provide the velocity and density information of subsurface layers respectively, are used. The DT is a delay time log and its inverse gives the velocity.

These logs are acquired in the borehole. We use this velocity and density data to compute a series of reflection coefficients called reflectivity series. Then a source Ricker wavelet with a dominant frequency of 10-30 Hz is generated. The reflectivity series is convolved with the source wavelet to get a synthetic seismogram (Figure 3.16). In this case we have performed the convolution with only one reflectivity series (1D), thus only one seismic trace is generated. Graphically we plot multiple copies to display it in the form of a stack section. The synthetic seismogram vertical units are meters or feet and it can be converted into time units by using its own velocity information. Synthetic seismogram is matched with the seismic section at the well point to correlate the succession of reflectors. It may also be used to calibrate our seismic velocities.

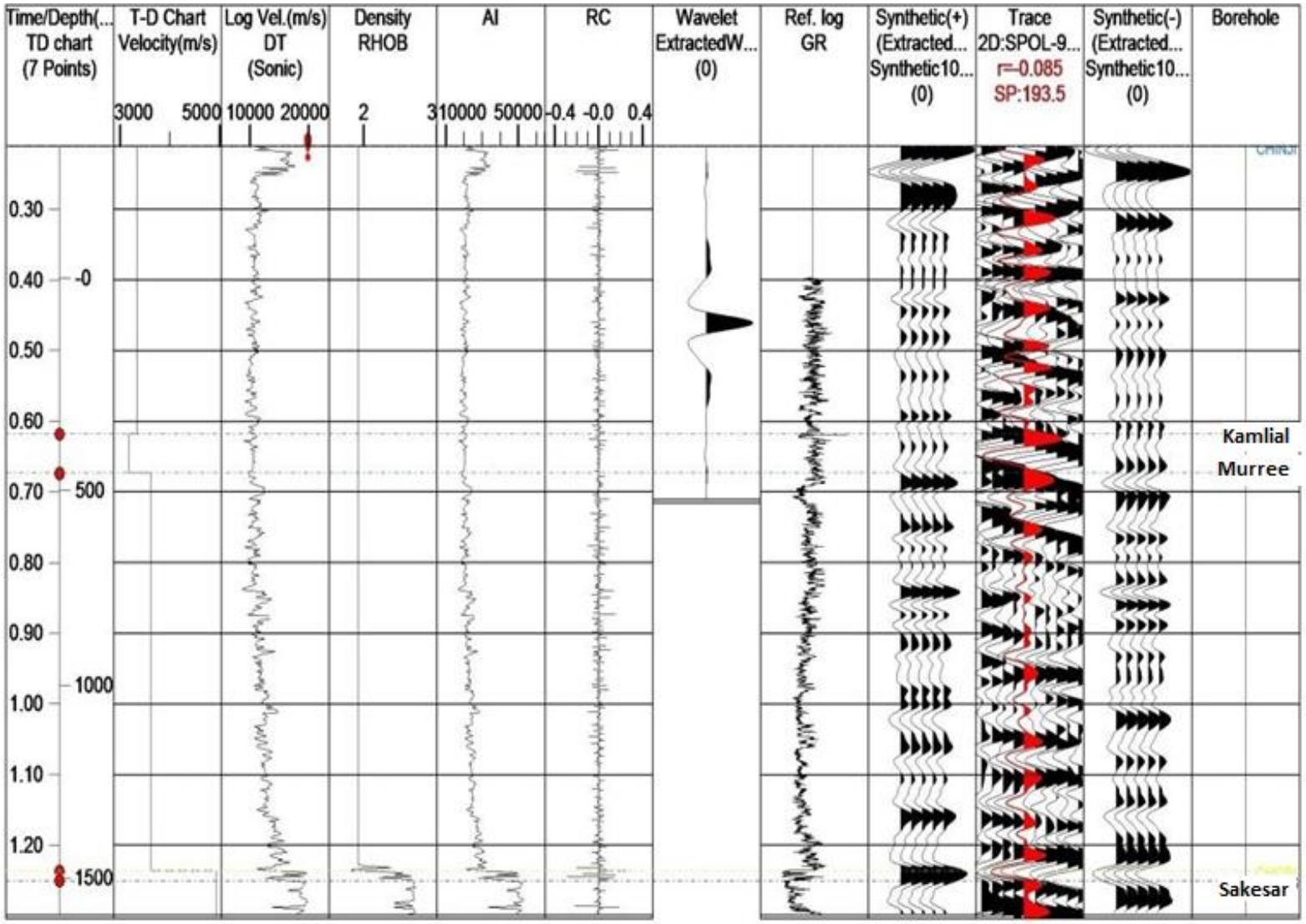

Fig 3.17: Synthetic seismogram generated on well Minwal-X

3.12 Seismic Attributes:

The Components of seismic date which are obtained by calculation are seismic attributes; seismic attributes are established in 1970s as a part of seismic interpretation. Any information that can be obtained from seismic is seismic attribute.

3.13 Why we need Attribute:

During the processing sequence we lose lot of information due to AGC (automatic gain control), Stacking (changes occur in frequency and amplitude) and deconvolation (trace are reshaped). Attribute are used to regain this information in a meaning display.

3.14 Classification of Attributes:

Attribute are classified into two major categories:

- *Physical attributes*
- *Geometrical attributes*

3.14.1 Physical Attributes:

Physical attributes are directly related to lithology, wave propagation etc. the physical attributes can be pre stack or post stack. The sub classes of physical attributes are instantaneous and wavelet. instantaneous attributes are evaluated at every instant of sample. the wavelet attributes show the characteristics of amplitude spectrum and characteristics of wavelet. Post stack attributes are obtained from stacked data.

3.14.2 Geometrical Attributes:

These attributes show discontinuous, dip, azimuth. The dip attributes is related to the dip of seismic events, as the dip makes the event clearer. The amplitude of the data on the data on azimuth attribute related to azimuth of maximum dip direction of the seismic feature.

3.15 The Trace Envelope

The trace Envelope is a physical attribute and it can be used as an effective discriminator for the following characteristics:

- Mainly represents the acoustic impedance contrast, hence reflectivity,
- Bright spots, possible gas accumulation
- Sequence boundaries
- Thin-bed tuning effects
- Major changes in depositional environment
- Spatial correlation to porosity and other lithological variations,
- Indicates the group, rather than phase component of the seismic Wave propagation.

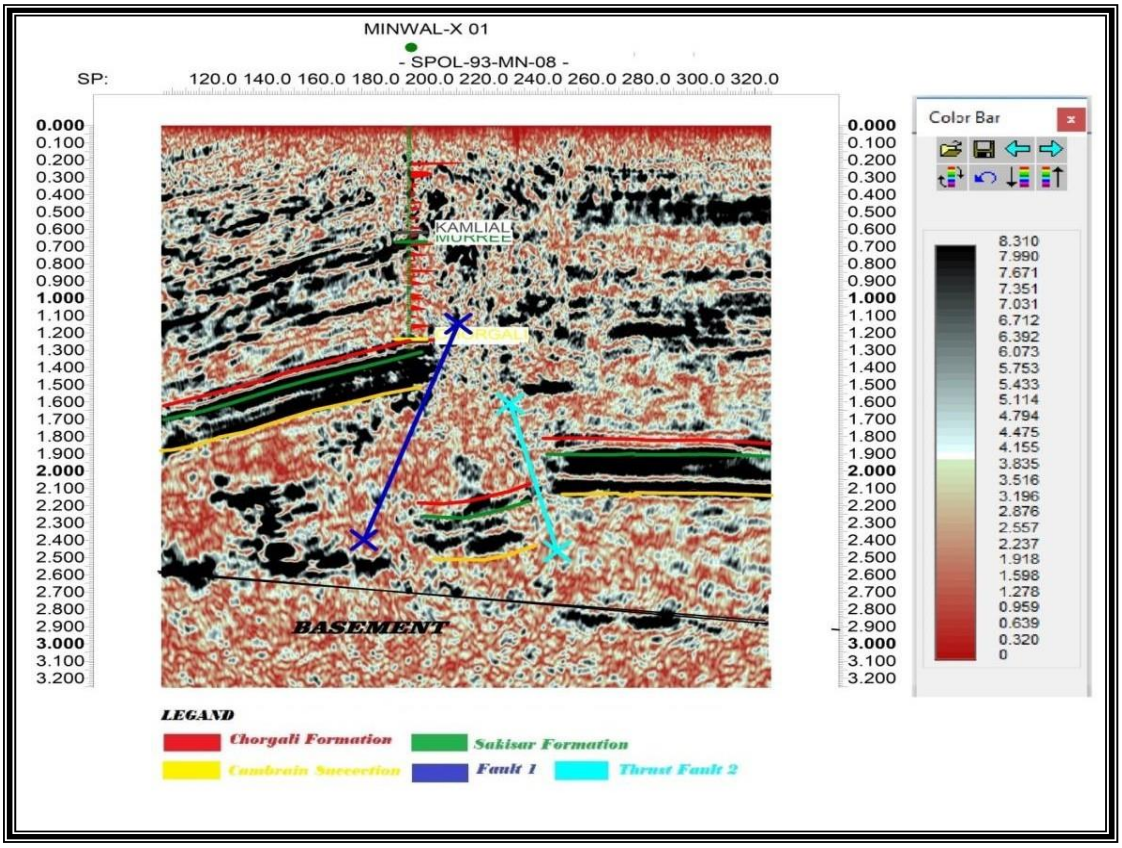

Fig 3.18 Trace Envelope of Line SPOL-93-MN-08

3.15 Relative acoustic impedance

It is a measure of acoustic impedance that lacks the background trend. It is the only seismic impedance attribute that can be computed directly from conventional post-stack seismic data. All other impedance attributes require additional data to supply missing low-frequency information. Relative acoustic impedance effects an integration of the

seismic trace. Integration rotates the phase of the trace by 90 degrees and boosts low frequencies relative to high frequencies (see figure below). Because low frequency signal is usually more coherent than high frequency signal, integration usually makes seismic data look cleaner within the bandwidth of the signal. However, integration also dramatically boosts low frequency noise, so it must be followed by a low-cut frequency filter to remove this noise.

3.16 Uses

Under favorable circumstances, relative acoustic impedance indicates differences in porosity. This rough empirical relation is not always valid, so impedance results should be calibrated with porosity logs to establish the relation wherever possible.

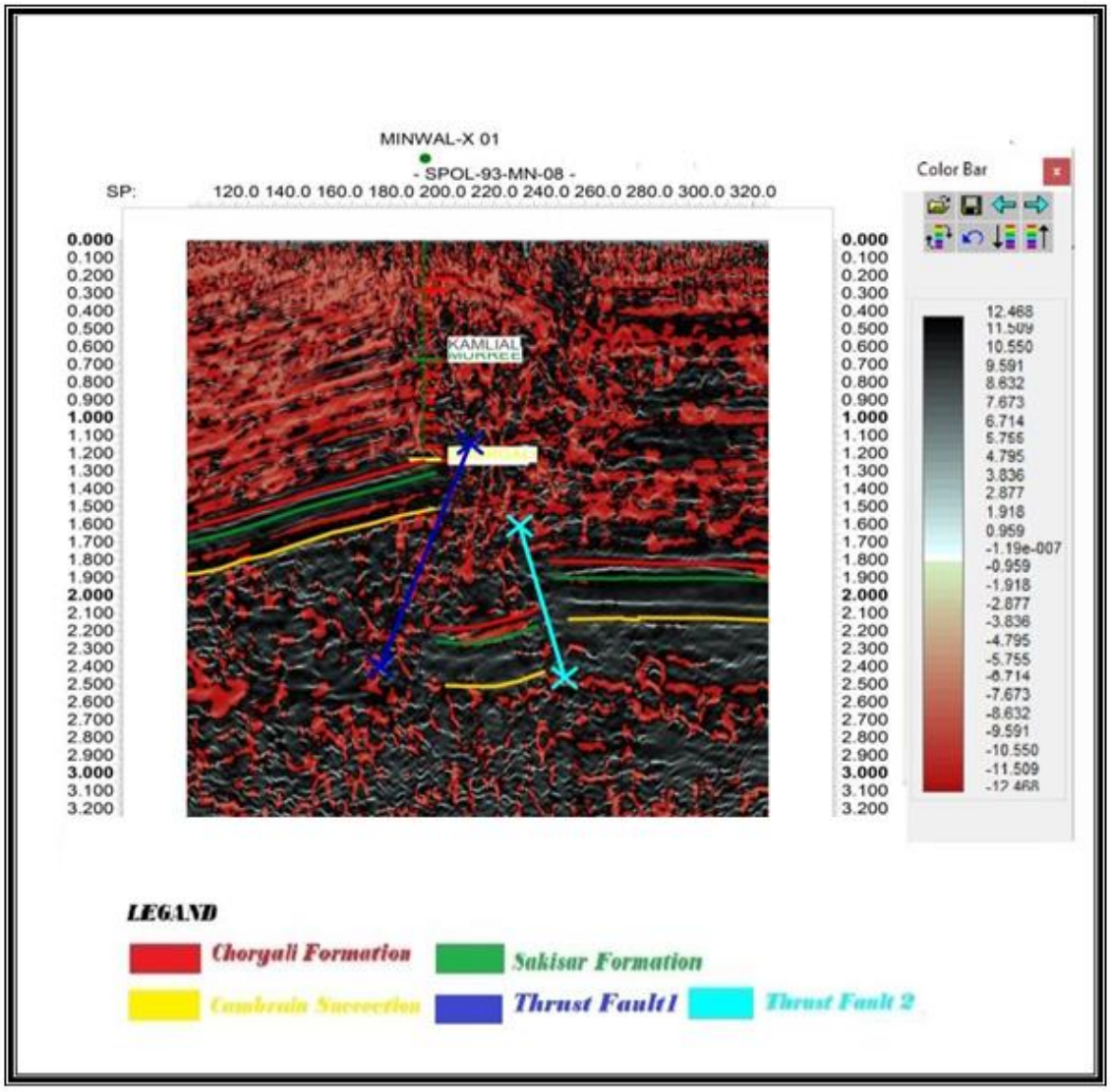

Fig 3.19. Relative acoustic impedance

3.17 Average Energy:

Average energy is a post-stack wavelet attribute, in which, within a specified window the square root of the sum of squared amplitudes is calculated and divided by their number of samples. The wavelet attributes are computed at the peak of the envelope, which represent the attributes of the wavelets within a zone defined by the trace envelope minima. These attributes indicate spatial variation of the wavelets and therefore relate to the response of the composite group of individual interfaces below the seismic resolution. The attribute has a blocky response and individually highlights the seal, reservoir and source rocks as shown in Figure.

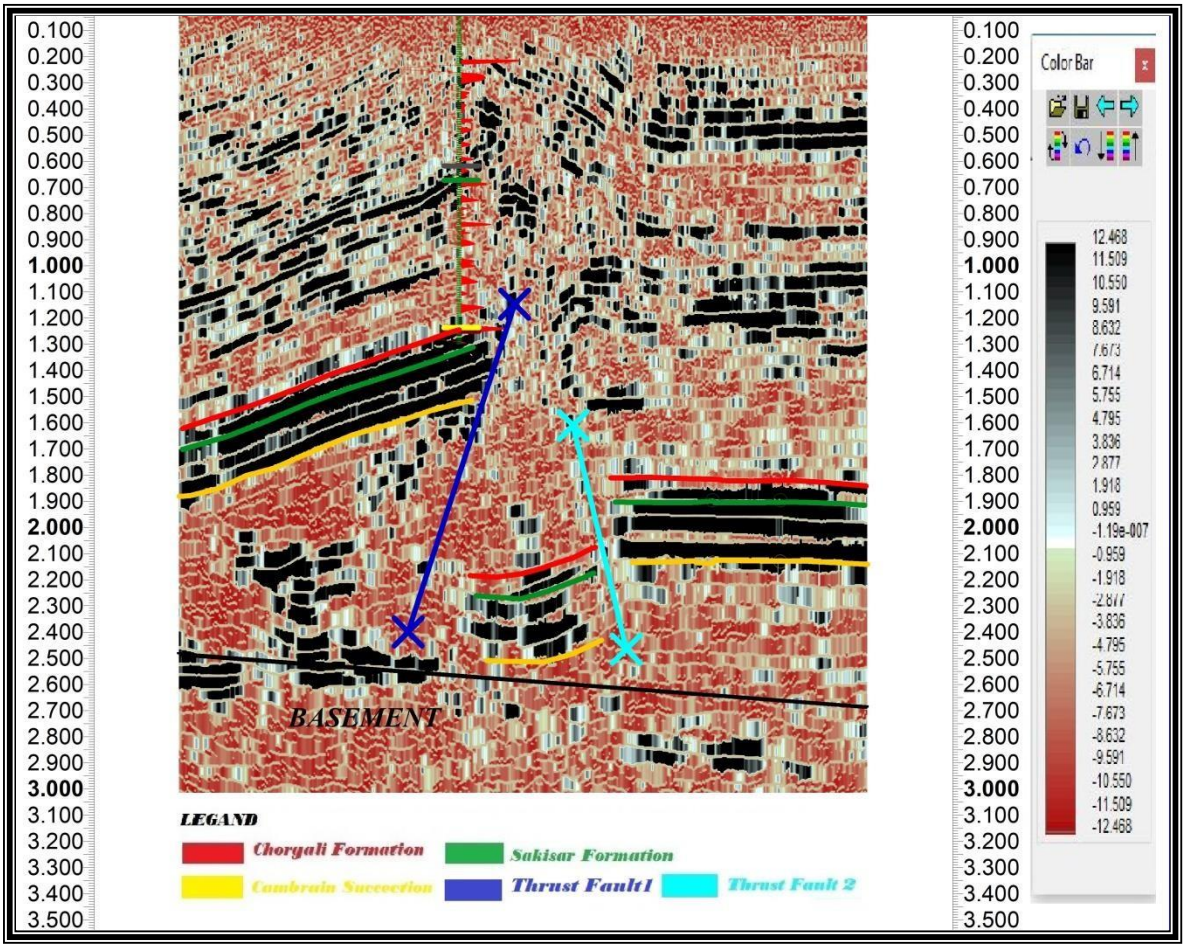

Figure 3.20: Average energy attribute calculated for seismic line

CHAPTER 04: PETROPHYSICAL INTERPRETATION

4.1 Introduction to Petro-physics

Petro physics deals with the study of the physical properties of naturally occurring rocks in relation to fluid movements within these rocks. These properties are porosity, permeability and density etc. Which have impacts on fluids movements within this rock. This chapter mainly focused on the petro physical properties and their use in reservoir modeling and reserves estimations. The main source to get petro physical properties of the sub surface rocks is to run wire line logs in exploration wells. These petro physical properties are used to detect and quantify the volume of hydrocarbons in the wells and then are implementing on whole area of interest. This science depends on negotiation. Amount of hydrocarbon in a formation, the quantity required, is not recorded by any log directly, instead are best guess by formula (Rider, 2002)

4.2 Well Logs Used in petro-physics are:

- Gamma Ray logs
- Deep Resistivity logs
- Sonic logs
- SP log

4.3 Flow chart of Petrophysices:

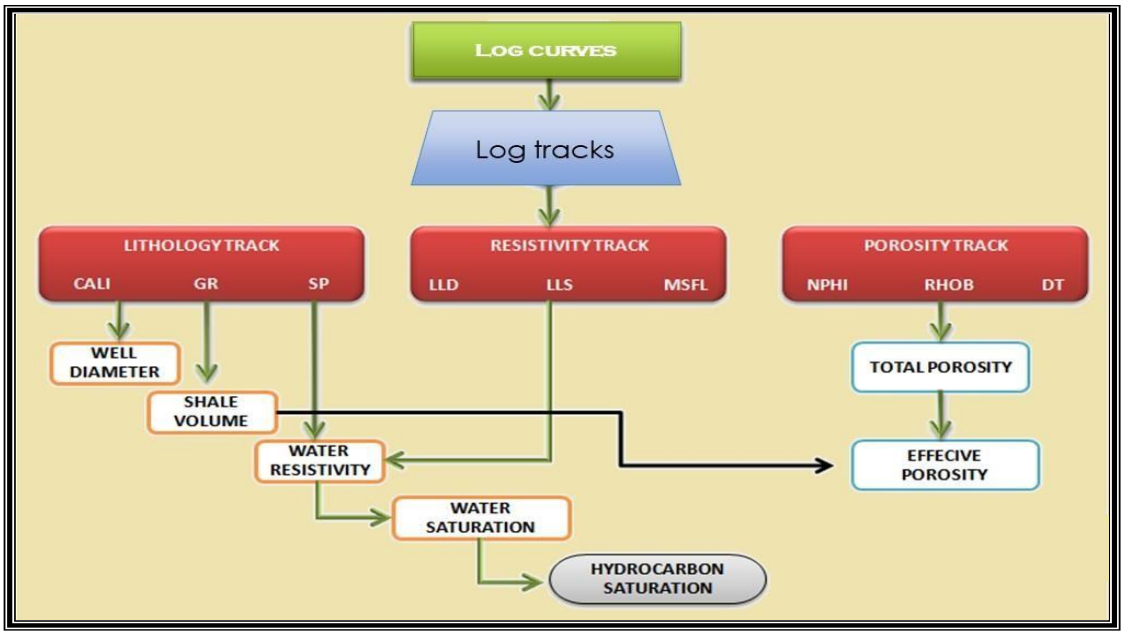

Fig 4.1: Flow chart for porosity calculation

4.4 Petro physical interpretation Logs

The following parameters are determined from these logs for petro physical interpretations:

- Volume of shale
- Porosity
- Resistivity of water in reservoir
- Water saturation
- Hydrocarbon saturation

The main hydrocarbon zone from where these hydrocarbons can be extracted volumetric estimation of hydrocarbons from both petro physical parameters and seismic grids of reservoir.

Main calculations of the concern logs are described in detail:

4.5 Volume of shale

The volume of shale present in subsurface formations can be calculated by using different logs. However, most of the logs have some ambiguities. We use Gamma-ray log for shale calculation. The mathematical calculation from gamma ray log for the volume of shale (Asquith and Gibson, 2004).

represents volume of shale, GRlog represent Gamma- ray log, represents minimum value of GR-log in that formation and GR shale represents maximum value of GR-log in that formation.

Mathematically can be proved by the formula (6.1).

- 1st we will take maximum value from the digitized GR log
- Then will take minimum value from the digitized GR log At the depth of which is start from (850 to 2150 m)

Maximum value = 100 Minimum value = 35

So average volume of shale is 50.3%

Which can be represented by the graph is given below

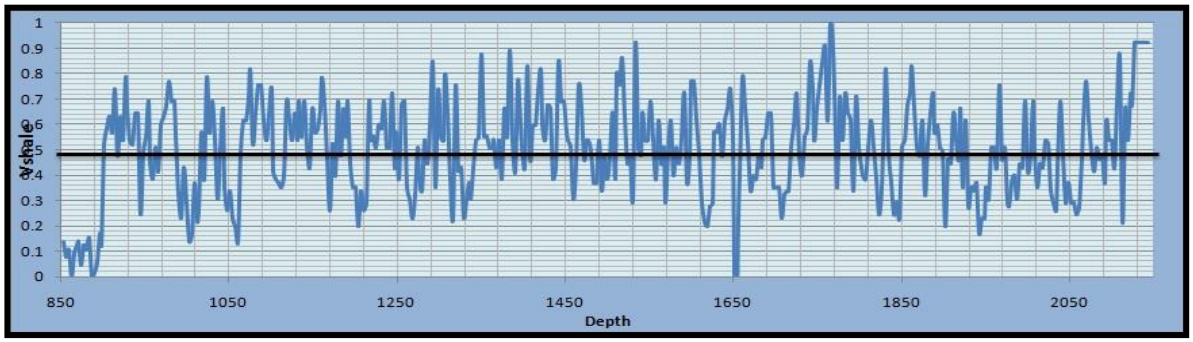

Fig: 4.2 show Reservoir and volume of shale graph

In figure 5.1 from "0" to "0.5" show the reservoir portion and from "0.5" to "1" on the is showing the volume of shale.

4.6 Calculation of porosity from logs:

The mathematical measurements of the ratio of pores spaces in a rock to the total volume of rock can be measured in (%). For finding the porosity we use the sonic log which is given by DGPC which start from "850" to "2150m" depth.

4.7 Average porosity

It is the sum of porosity obtained from different logs divide by the number of logs from which porosity is determined.The relation from which average porosity is calculated is given below:

Acoustic logging tools can assist in evaluating porosity because the compression velocity of sound in fluid is less than the velocity in rock. If there is pore space in the rock, and it is fluid-filled, the acoustic energy will take longer to get from the transmitter to the receiver (i.e., low velocity indicates high porosity).

The velocity of most borehole and reservoir fluids (except gas) does not vary greatly:

- A fluid velocity (Δt_f) of 189 μsec/ft (5,300 ft/sec) is generally assumed for fresh drilling fluids
- A slightly lower value, 185μsec/ft, is used for salt muds is equal to 47.6

Fluid type becomes more of a concern when oil-based mud (OBM) is used if the formation of interest is not invaded or if invasion is very shallow. The lithology must be known or estimated in order to select the appropriate matrix velocity.

The Wyllie equation represents consolidated and compacted formations. In poorly consolidated or unconsolidated rocks, a correction factor is necessary (**Eq. 5**). Also, the presence of shale or clay within the sand matrix will increase Δ t by an amount proportional to the bulk-volume fraction of the clay. An empirical equation is used for calculating porosity in sandstones in which adjacent shale values (Δt_{sh}) exceed 100 μsec/ft (**Eq. 6**):

$$\phi = \frac{\Delta t - \Delta t_{ma}}{\Delta t_f - \Delta t_{ma}} \times \frac{1}{C_p}, \qquad \text{Equation (4.1)}$$

Where the compaction correction factor C_p is

$$C_p = \frac{\Delta t_{sh}(C)}{100}, \qquad \text{Equation (4.2)}$$

where

Δt_{sh} = specific acoustic transit time in adjacent shales (μsec/ft), 100 = acoustic transit time in compacted shales (μsec/ft)

$$\phi = \frac{\Delta t - \Delta t_{ma}}{\Delta t_f - \Delta t_{ma}}$$

So, the Average porosity can be calculated by this formula:

So, by putting the values the average porosity is equal to 29% which can be represented by a graph also

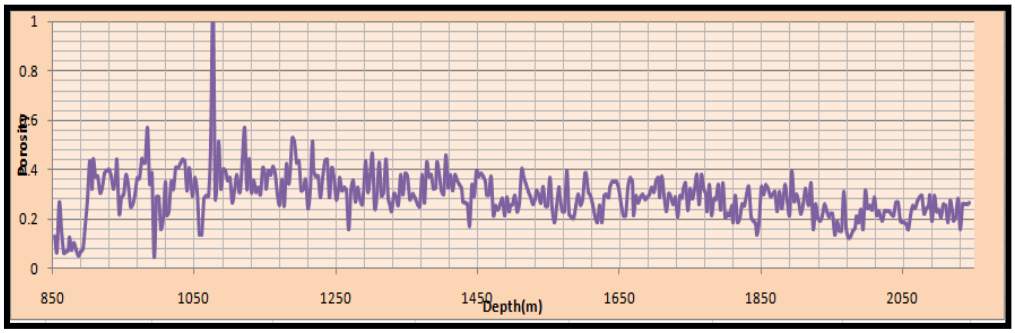

Fig:4.3 show porosity

4.8 Effective porosity

The effective porosity is the percentage of interconnected pore space with respect to the bulk volume. The effective porosity is the value that is used in calculations because it represents the interconnected pore spaces that contains the recoverable hydrocarbon fluids. Effective porosity can be found by the formula

Rock Property	Mathematical Equation
Volume of Shale	Vshl[] = min(1, max(0, (GR[]-GRcln) / (GRshl-GRcln)))
Density Porosity	PHID[] = (RhoM - RHOB[]) / (RhoM - RhoF)
Average Neutron Density Porosity Effective Porosity	PHIA[] = (PHID[] + PHIN[]) / 2 PHIE[] = PHIA[] * (1-Vshl[])
Archie Water Saturation	SwA[] = sqrt(Rw / (LLD[] * PHIA[]^2))
Hydrocarbon Saturation	Hc = 1-Sw

Table 4.1: Different equations for calculating rock properties (Asquith et al., 2004)

So, by putting the value the effective porosity is equal to 13% which can be also represented by a graph (5.4)

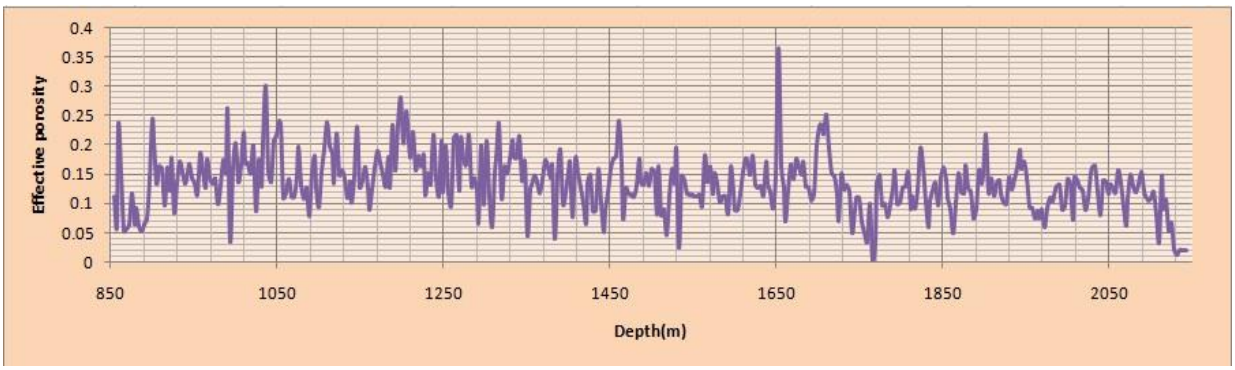

Fig:4.4 : Describe the Effective porosity

4.9 Resistivity of Water

The resistivity of water can be calculate by applying certain tests for the selected area or formation, the first test for calculating the resistivity directly then pass current between the electrodes on the logging tool and the potential drop between that electrodes gave us the resistivity. The second test is the indirect measurement by measuring the conductivity by inducing current in the specified formation through the borehole and its capacity to carry current is observed. And at last taking its inverse so the resistivity should be calculated (Krygowski,2003). These tests gave the actual result of both fluid in pores and matrix. For

finding the resistivity of water or fluid some other tests may performed in steps these steps are given below Formation water resistivity (Rw) is calculated by knowing certain parameters i.e. static Spontaneous potential(SSP), resistivity of mud (Rmf1) at ground surface temperature (ST), Formation temperature, borehole temperature (BHT) water salinity, resistivity of mud (Rmf2) at formation temperature (FT).

4.10 Water saturation

Saturation is defined as that fraction or percent of pore volume occupied by water. The remaining fraction containing oil or gas is termed as hydrocarbon saturation (Sh) which is equal to 1-Sw.

Water saturation can be determined with the help of Archie‟s equation:

$$s_W = \sqrt{R_w / R_t * \emptyset_a^2}$$

Archie‟s equation

Where,

represent water saturation, represent porosity, represent Formation water resistivity, represent Observed LLD curve(resistivity of true zone), a represent Tortuosity factor (constant 1), m represent cementation factor (2 more or less)

For the evaluation of water saturation, first, we determine the water resistivity of the

formation, with the help of GEN charts. The value of evaluated is kept constant along with the values of other two constants and throughout the packages. These parameters are placed into the Archie‟s equation, along with the value of, which is the true resistivity of the formation to determine water saturation.

So water saturation can be finding by putting the value in Archie‟s equation is given below.

Water saturation can also be represented by a graph as shown in figure 5.8.

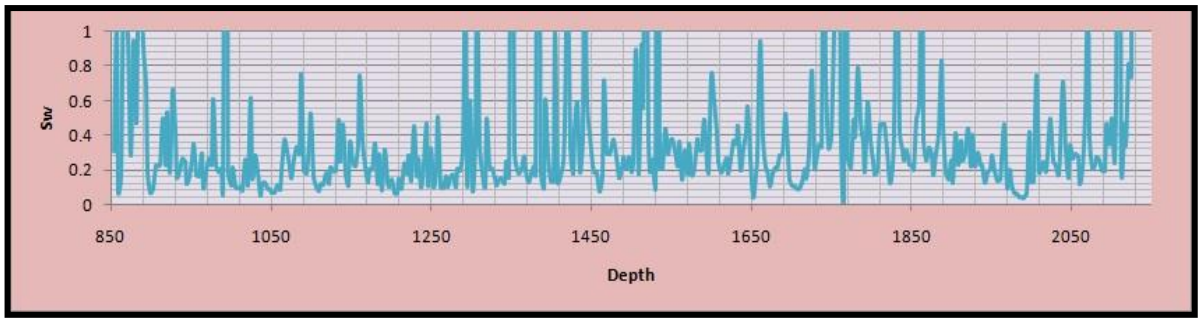

Fig.4.5 Water saturation can also be represented by a graph

4.11 Saturation of hydrocarbon

The fraction of pore volume filled with hydrocarbon. It is calculated by the following formula:

where;

Sh denote Saturation of hydrocarbon, Sw denote Saturation of water, So saturation of Hydrocarbon can be calculated from the equation (6.10.1)

By putting the value:

It can also be represented by a graph as shown in figure 5.9.

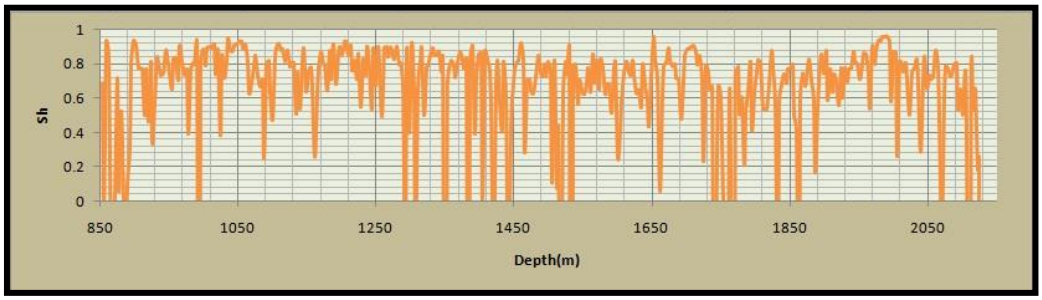

Figure: 4.6 saturation of Hydrocarbon

Fig.4.7: COMBINE GRAPH OF, PEROSITY, EFFECTIVE POROSITY,

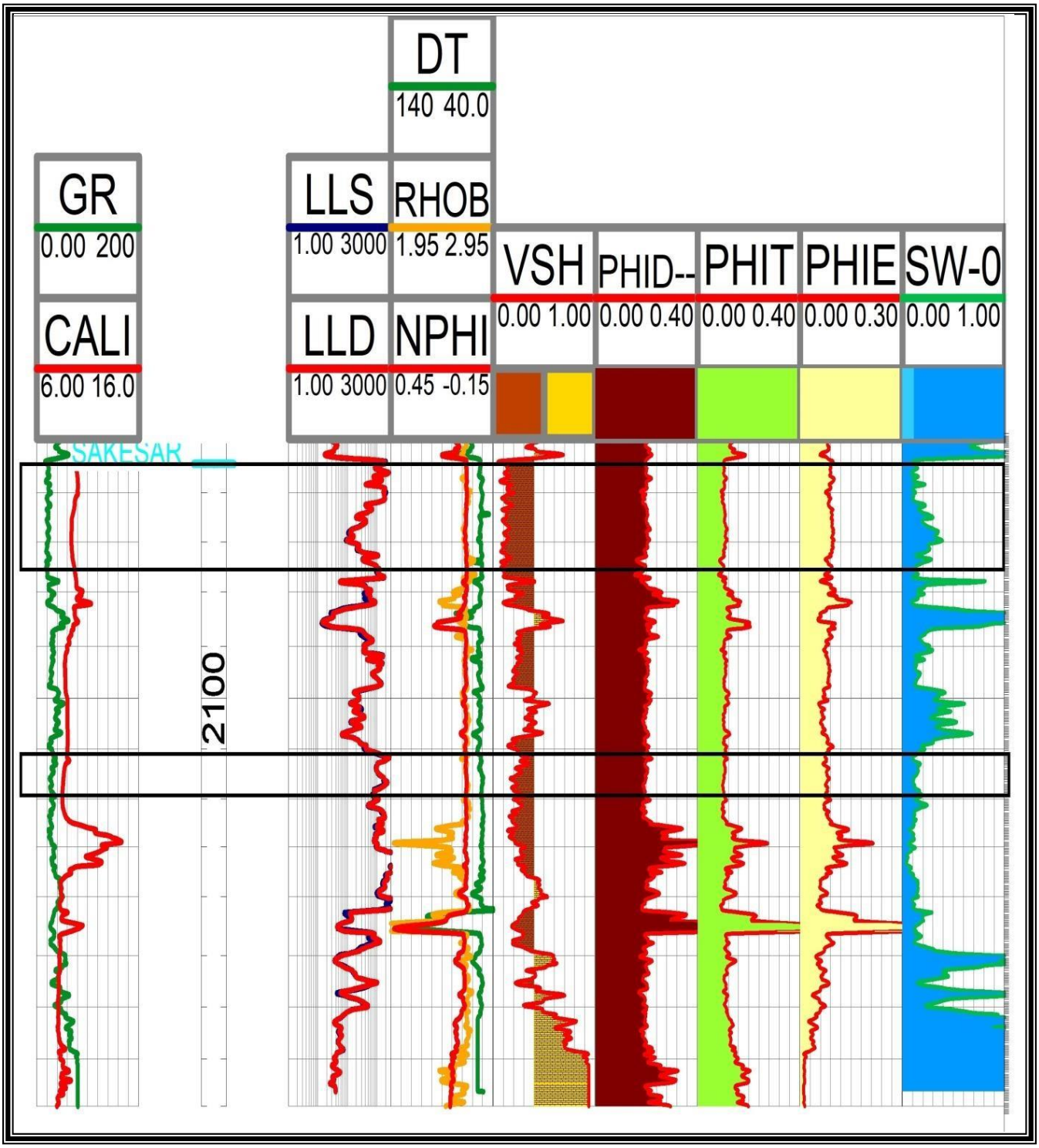

4.8. Petro-physical Report of Joya Mair oil field of Minwal X-01 Well, while boxes on the figure are showing the good prospecting zones.

Different Petro-physical properties obtain from the Logs are

4.12 Chorgali Formation

Petrophysical properties	Percentage (%)
Average Volume of shale	50.3%
Average porosity PHIT	30%
Effective porosity PHIE	13%
Average water saturation SW	33.19 %
Average Hydrocarbon saturation SH	66.8 %

4.13 Facies Modeling

Facies are generally considered as bodies of rocks that show some specific characters but ideally these are rock units that form under certain conditions of sedimentation, displaying a particular process or environment of deposition. Facies models provide additional aid to the understanding of sedimentary environments and the origin of old sedimentary rocks. Different models can be made to explain a given set of data, depending on which aspect of the facies should be highlighted most to get much information about it.

In linked with petrographical and lithological variation different kinds of facies are identified on the basis of structure, composition and sedimentary texture (Ahmad et al., 2002). Different types of sedimentary environments are known like Continental sedimentary environment that include glacial, alluvial fan, river channel, flood plain, aeolian, and dunes environments. Transitional (shoreline) environment include delta, beach, Barrier Island, lagoon and tidal flat environments. Marine environment include coral reefs and submarine facies. Each unit (facies) possesses a distinctive set of characteristics reflecting the conditions in a particular environment. The facies types reflect high-energetic and low-energetic hydrodynamic conditions that are either related to gradually increasing water depths or are produced by superimposed high-energy

events, for instance, during storms. The famous law about the deposition of sediments is the Walther‟s law that is briefly explained.

4.14 Walther's law of Facies

Walther's Law of Facies states that the vertical succession of facies displays lateral changes in environment. Conversely, it states that when a depositional environment “migrates" laterally, sediments of one depositional environment come to lie on top of another. A classic example of this law is the vertical stratigraphic succession that typifies marine transgressions and regressions that are briefly explained. However, the law is not applicable where the contact between different lithologies is non-conformable.

Transgression: A marine transgression is a geologic event during which sea level rises relative to the land and the shoreline moves toward higher ground, resulting in flooding.

Regression: A marine regression is a geologic event during which sea level falls relative to the land and the shoreline moves toward lower ground and exposes former sea bottom.

Three combinations have been recognized on the basis facies analysis given below:

- Lowe energy facies consisting of cross bedded sandstone, thin bedded sandstone and grey shale, massive sandstone and pelagic lime mudstone.
- Moderate energy facies consisting of laminated sandstone and grapestone.
- High energy facies consisting of interbedded gypsiferous shale and siltstone/sandstone and bioclastic grainstone (Ahmad et al., 2002).

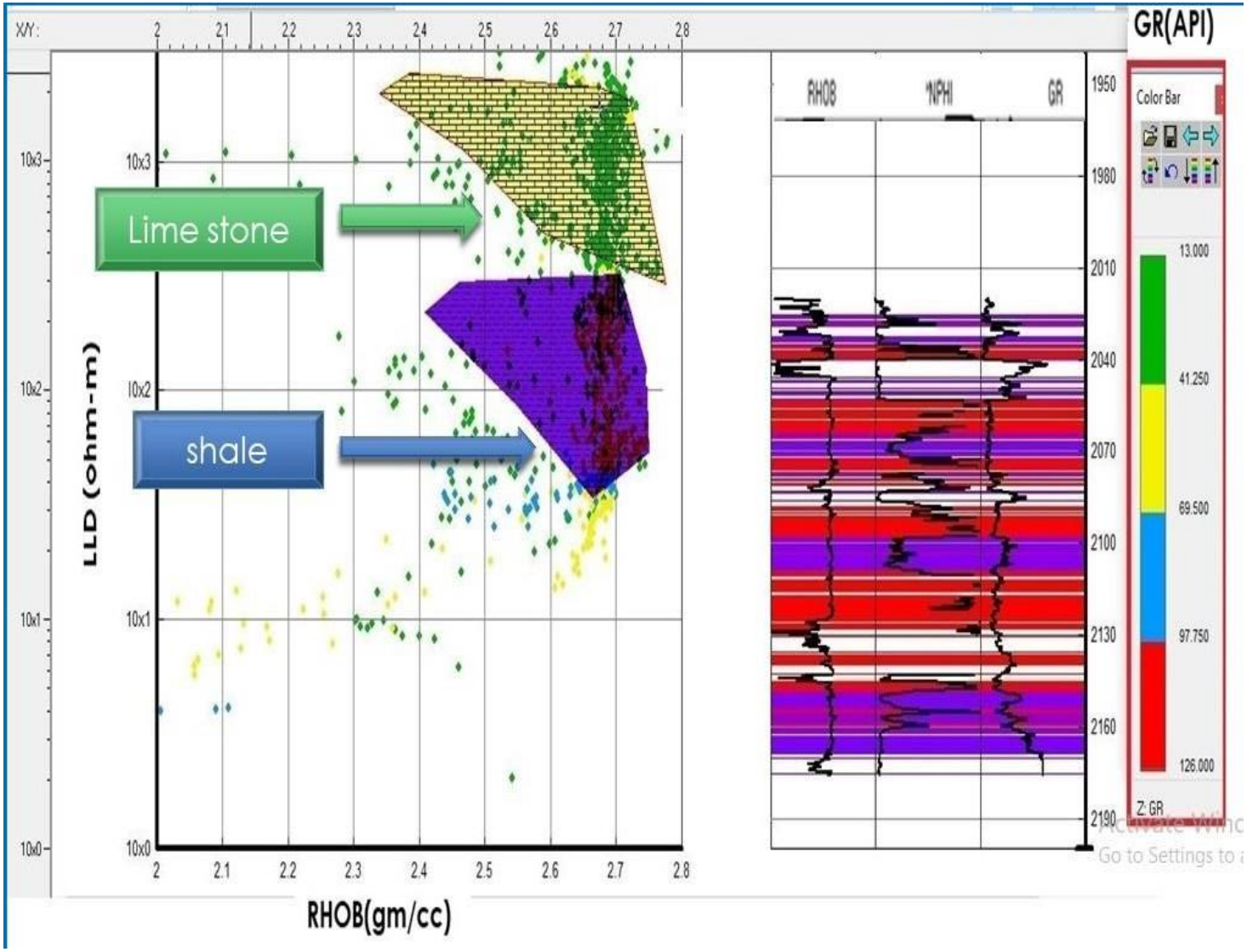

Fig 4.9 facies analysis of joya mair oil field

CHAPTER NO 5 GASSMANN FLUID SUBSTITION:

5.1 Introduction

Fluid substitution is an important part of seismic rock physics analysis (e.g., AVO, 4-D analysis) which provides a tool for fluid identification and quantification in reservoir. This is commonly performed using Gassamann‟s equation (Gassmann, 1951). Many authors (Batzle and Wang, 1992; Berryman, 1999; Wang, 2001; Smith et al., 2003; Russell et al., 2003; Han and Batzle, 2004) have discussed the formulations, strength and limitations of the Gassmann fluid substitution (Kumar 2006).

5.2 Gassmann's Fluid Substitution

Saturated porous reservoir rock contains fluid and rock matrix. Porous rock is called dry rock, when there is no fluid in pores. Production of oil from a reservoir affects the fluid part and does not affect solid part. Kumar (2006) describes these fluctuations affect as the elastic constants (bulk modulus (K), shear modulus and density etc, which affects the velocity of seismic wave. K of dry and water saturated rocks are more sensitive to water saturation than P wave velocity under same condition of pressure (Batzle and Wang, 2004)). Furthermore, water saturation has slight effects on μ, as shear modulus of fluid is zero. Gassmann‟s model calculates and of saturated rock by computing K, μ and ρ for saturated reservoir rock, in order to efficiently replicate effects of fluid substitution. The objective of fluid substitution is to model the seismic properties (seismic velocities) and density of a reservoir at a given reservoir condition (e.g., pressure, temperature, porosity, mineral type, and water salinity) and pore fluid saturation such as 100% water saturation or hydrocarbon with only oil or only gas saturation (Kumar, 2006). Seismic velocity of anisotropic material can be estimated using known rock moduli and density. P- and S-wave velocities in isotropic media are estimated as,

Respectively, where and are the P- and S-wave velocity, K and are the bulk and shear moduli, and is the mass density. Density of a saturated rock can be simply computed with the volume averaging equation (mass balance). Other parameters required to estimate seismic velocity after fluid substitution is the moduli and which can be computed using the Gassmann‟s equations.

5.3 Gassmann's Equations

Gassmann‟s equations relate the bulk modulus of a rock to its pore, frame, and fluid properties as

Where, and are the bulk moduli of the saturated rock, porous rock frame (drained of any pore-filling fluid), mineral matrix, and pore fluid, respectively, and is porosity (as fraction). In the Gassmann formulation shear modulus is independent of the pore fluid and held constant during the fluid substitutions. Bulk modulus and shear modulus (μ) at in-situ (or initial) condition can be estimated from the wire line log data (seismic velocities and density) by rewriting equations 1 and 2 as

5.4 Gassmann Fluid Substitution Wizard via Kingdom Software

The Gassmann Fluid Substitution Wizard uses Gassmann‟s theory to create new velocity and density logs. Gassmann‟s theory describes seismic wave propagation in fluid-saturated porous solid using mathematical relationships between various properties of the rock skeleton (the solid material) and the fluid filling the pore space.

There are three steps to completing Gassmann‟s wizard:

Step 1.

Select a well, borehole, and porosity source (Figure 5.1).

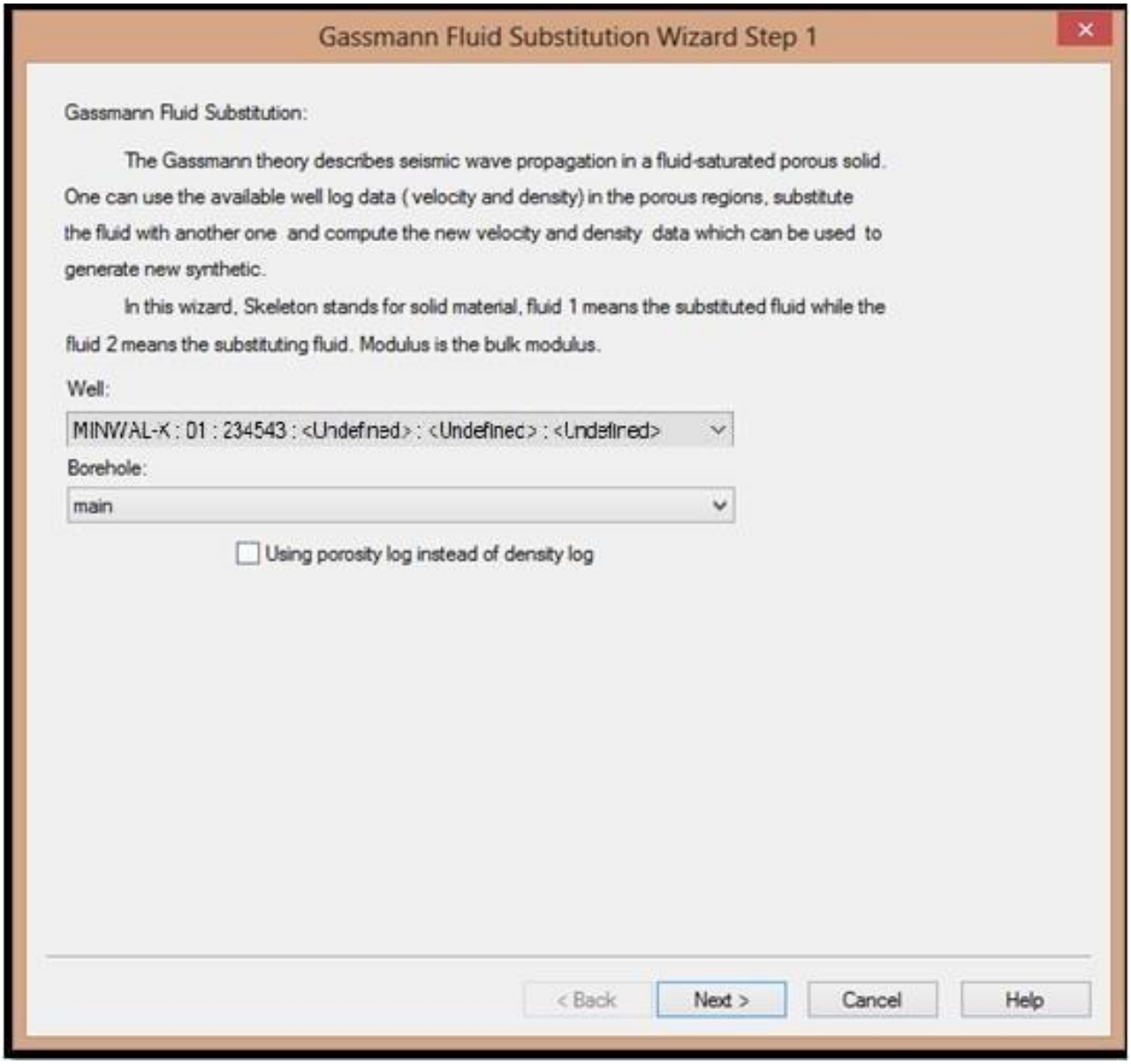

Figure5.1: Window of Gassmann's Substitution First step

As the Minwal X-01 is producing well, so we select that well for Fluid Substitution.

Step 2.

Select the density/porosity and velocity logs, define the skeleton and fluid parameters, and digitize the substitution regions (Figure 5.2).

5.4.1 Gassmann Fluid Substitution Fluid Parameters as Water and Gas

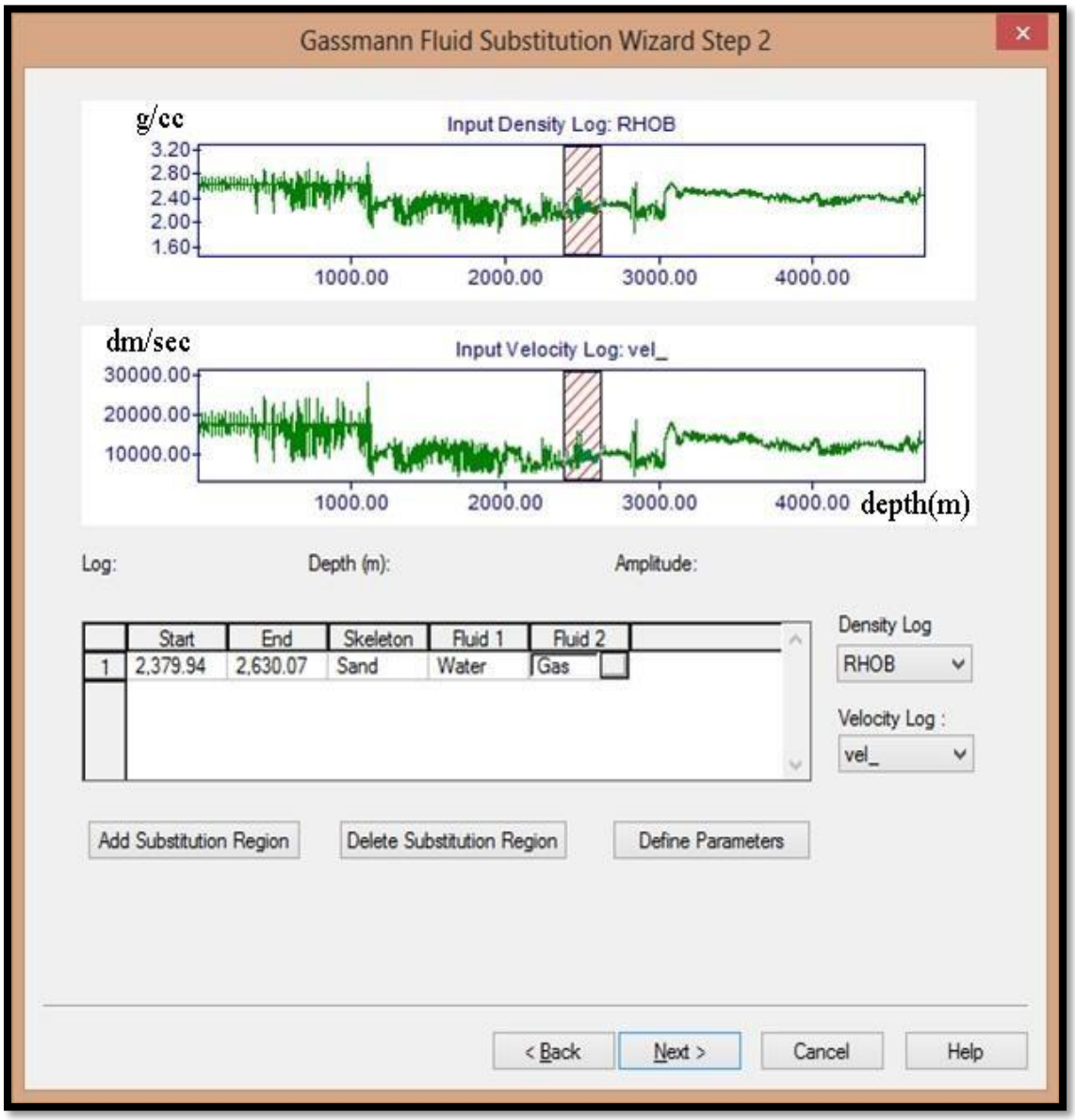

Figure5.2: Window of Gassmann's Fluid Substitution second step

As mention earlier, in this step we input the density and velocity log of the Siraj South well. Then I mark the probable prospective zone (Lower Guru formation thickness) which acts as reservoir for hydrocarbon accumulation. After that we define the parameters (density and bulk modulus) of skeleton and types of fluid present in reservoir rock

By clicking<Next> in the windows, we get the computed density and velocity log (Figure 5.3).

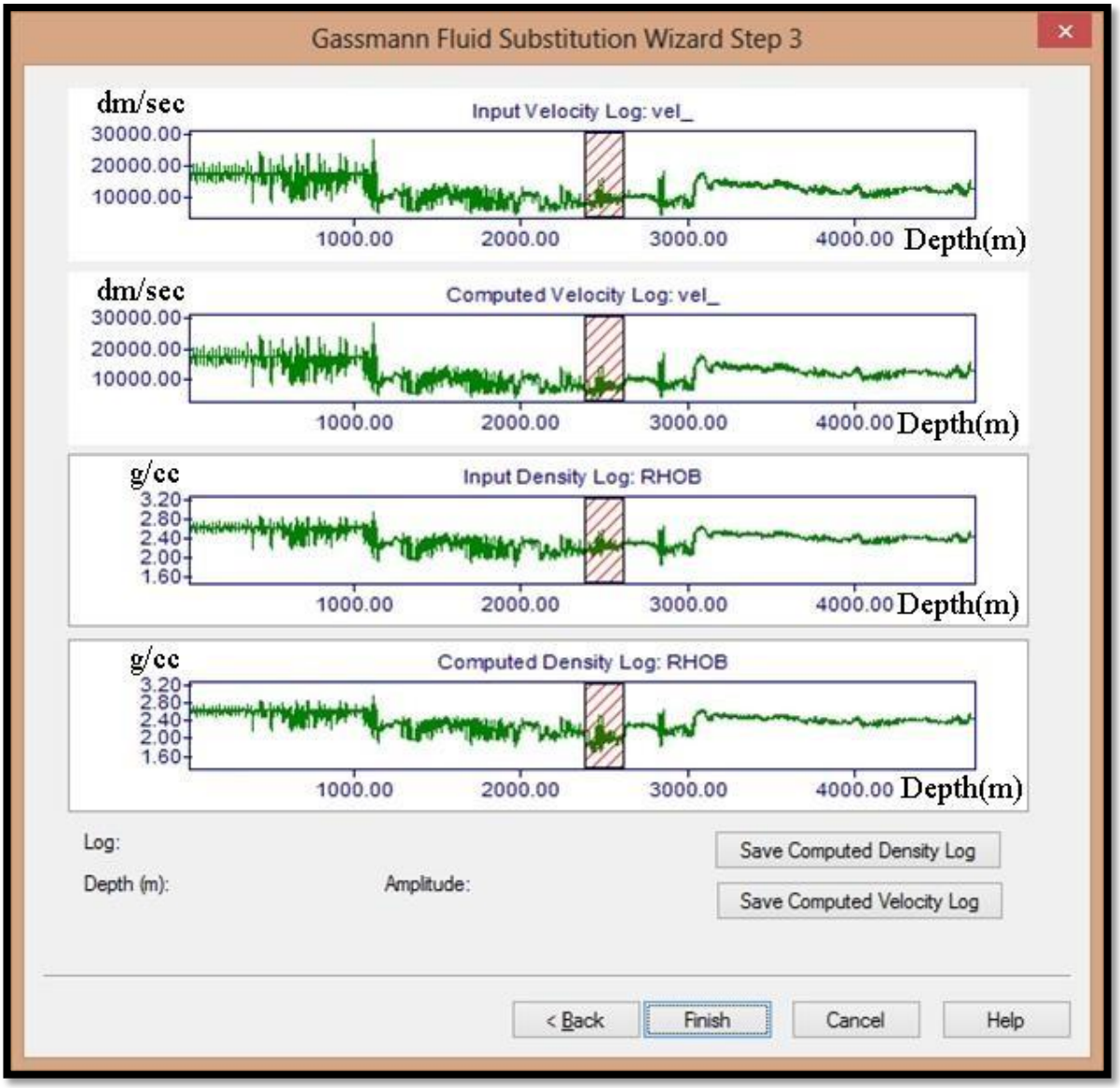

Figure5.2: Input and computed velocity and density logs (for fluid as water and gas) Step 3.

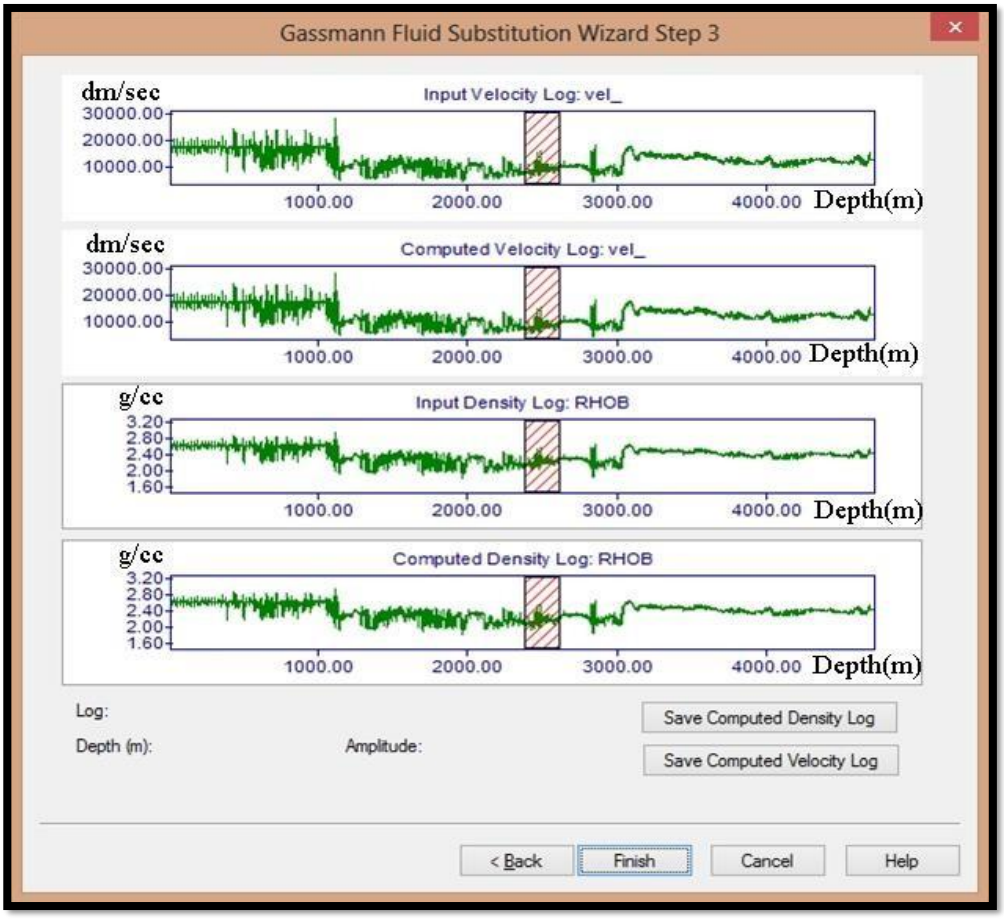

Figure5.3: Input and computed velocity and density logs (for fluid as water and oil)

Variation in density and velocity is shown in Figure 5.3 due to Gassmann Fluid Substitution theory.

5.5 Results of Gassmann Fluid Substitution

We can clearly see that after applying the Gassamann‟s fluid substitution, there decrease in density and velocity in the marked zone. When fluid parameters are water and oil there is more decrease in density and velocity (Figure 5.2) as compared when fluids are water and oil (Figure 5.3). This is because density of gas is less than oil, so velocity of waves is low in gas medium. We can generate more computed curve by changing the water saturation level and other fluids in the reservoir zone can estimate the amount of hydrocarbon present in the reservoir at different water saturation level. These log curves help in the drilling of development wells. These new logs can also be saved and used to generate a new synthetic seismogram, which shows better results.

CHAPTER NO 6 COLORED INVERSION

6.1 Wavelet and Acoustic Impedance:

For many seismic processing applications, it becomes necessary to derive an estimate of the seismic wavelet. Because the character of wavelet is imprinted on seismic traces, it is important to understand its shape in order to decipher the properties of earth's interior from seismic traces. Despite the fact the wavelet is time varying and is expected to be spatially varying, an overall knowledge of wavelet is crucial to enhancing resolution for better imaging of structure and predicting lithology and fluid content. The most common practice is to invert post-stack seismic data for wavelets. A post-stack trace emulates a zero-offset or normal-incidence seismogram, which can be simulated using convolution model assuming 1D earth model. Most seismic data contain noise this problem must be compensated. In frequency domain, the convolution operation is replaced by a multiplication. Three inverse problems are identified. Estimation of the wavelet when the reflection co-efficient is known. Estimation of reflection co-efficient or acoustic impedances when the wavelet is known. Simultaneous inversion for acoustic impedance of wavelet. Inversion of seismic data to Acoustic Impedance is usually seen as a specialist activity, so despite the publicized benefits, inverted data are only used in a minority of cases. To help overcome this obstacle we aimed to develop a new algorithm which would not necessarily be best in class but would be quick and easy to use and increase the use of inversion products within BPA. This new technique, Colored Inversion performs significantly better than traditional fast-track routes such as recursive inversion, and benchmarks well against unconstrained sparse-spike inversion.

Once the Colored Inversion operator has been derived it can be simply applied to the data on the interpretation workstation as a user-defined filter. In this way inversion can be achieved within hours since the volume data do not have to be exported to another package, and no explicit wavelet is required. The inversion is understood simply by this flow chart shown in figure 6.1.

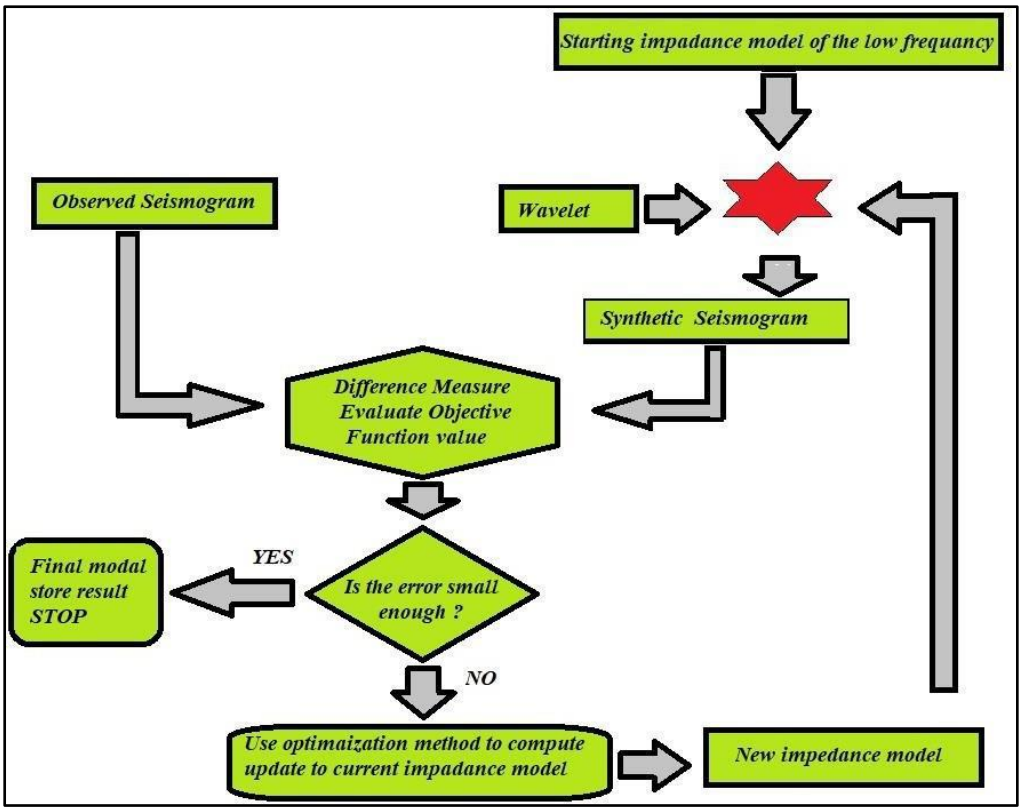

Fig 6.1 show the impedance and wavelet extraction workflow

6.2 Methodology:

- The well data and information of logs is required for the performing the colored inversion in Kingdom Software.
- The velocity is obtained from sonic log and density is obtained from density log and values of densities are obtained from density log by convolving these values.
- We get acoustic impedance by cross matching these impedance data with the input reflection data
- We derive a single optimal matching filter Figure (6.8). Convolving this filter with the input data we see in figure (6.7) that the result is very much similar, everywhere.
- This Empirical observation indicates that inversion can be approximated with a simple filter and that it may be valid over a sizeable region.

- The phase of the operator is a constant -90o which is in agreement with the

simplistic view of inversion being akin to integration, and the concept of a zero-phase reflection spike being transformed to a step AI interface, provided the data are zero-phase.

- Walden & Hoskins (1984) empirical observation tells us that earth reflection coefficient series have spectra that exhibit a similar trend that can be simply described as constant function. The term is a positive constant and is frequency arrives at a similar observation theoretically may vary from one field to another but tends to remain reasonably constant with in any one field (Velzeboer 1981).

- It therefore follows that if our seismic data are inverted correctly, they too should show the same spectral trend as logs in the same area.

6.3 Non-Uniqueness and Convolution:

The process of convolution for constructing a seismogram using a wavelet and acoustic impedance is performed to generate an operator. Note that wavelet is smoothly varying function, while the reflectivity is a series of delta functions placed at two-way normal time of each reflector (Cooke and Schneider 1983). The spectra of the wavelet and reflectivity series for synthetic are also shown in figure. We observe that wavelet is a band-limited, while reflectivity series is a broad-band. Because the convolution is equivalent to multiplication in frequency domain the spectrum of resulting seismogram is band-limited as well. We can imagine the complexity of the problem further we can take into account the loss of high frequencies of wavelet caused by attenuation. In other words, series cannot be assumed to be stationary. Even under stationary conditions the data does

Not contain all the frequencies. The most common approach to deriving the wavelet is based on well-log data that produce a true reflectivity series.

6.4 Wavelet Extraction:

The wavelet is shown in figure (6.2) is extracted on the basis of the well log data that provides the true reflectivity series (i.e. compressional wave velocity and density computed into acoustic impedance logs, which are mapped into normal incidence reflectivity series). An initial guess of wavelet is convolved with reflectivity series and

synthetic normal incidence trace is generated. The difference between the observed and synthetic traced is minimized using a suitable chosen norm with smoothness constraints (Sen and Stoffa, 2013).

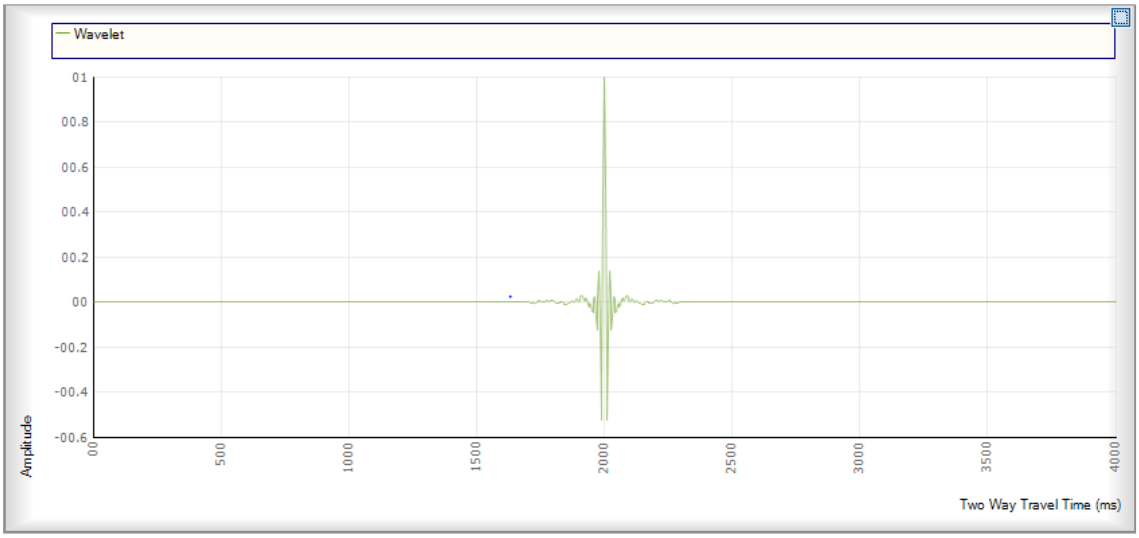

Fig (6.2): Extracted Wavelet

6.5 Impedance Estimation:

Now our approach is to convolve this wavelet with acoustic impedance (reflectivity series). The acoustic impedance is also computed from well log data as described previously. The impedance spectrum is shown in figure (6.3) is estimated after removing source wavelet; noise must be absent; all multiple reflections must be removed; spherical spreading including all plane reflections (Ghosh 2000).

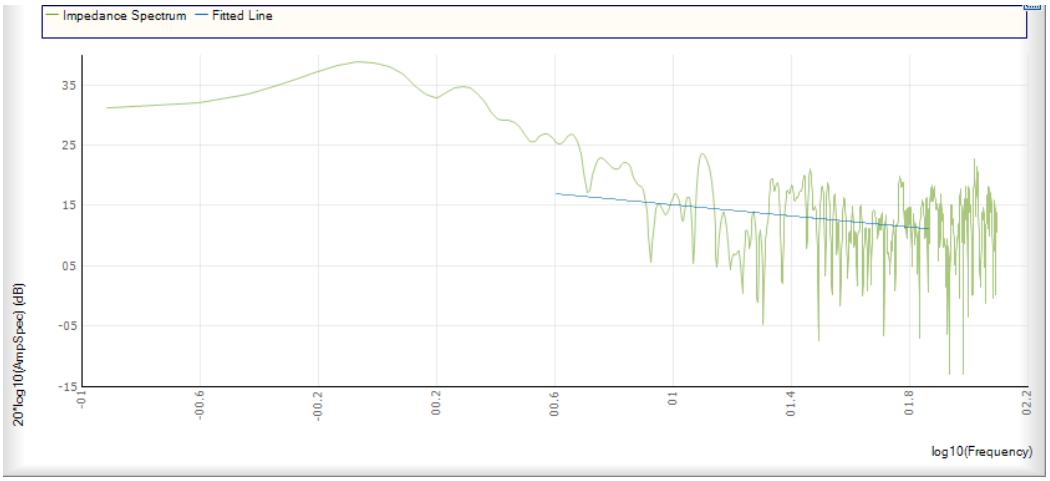

Fig (6.3): Impedance spectrum with fitted line.

6.6 Butterworth Filters:

The Butterworth filter is a type of signal processing filter designed to have as flat a frequency response as possible in the pass band. It is also referred to as a maximally flat magnitude filter. It was first described in 1930 by the British engineer and physicist Stephen Butterworth in his paper entitled "On the Theory of Filter Amplifiers.

An ideal electrical filter should not only completely reject the unwanted frequencies but should also have uniform sensitivity for the wanted frequencies. This filter is used here for convolution of the wavelet and reflectivity series for formulation of seismogram. The Butterworth filter is shown in figure (6.4).

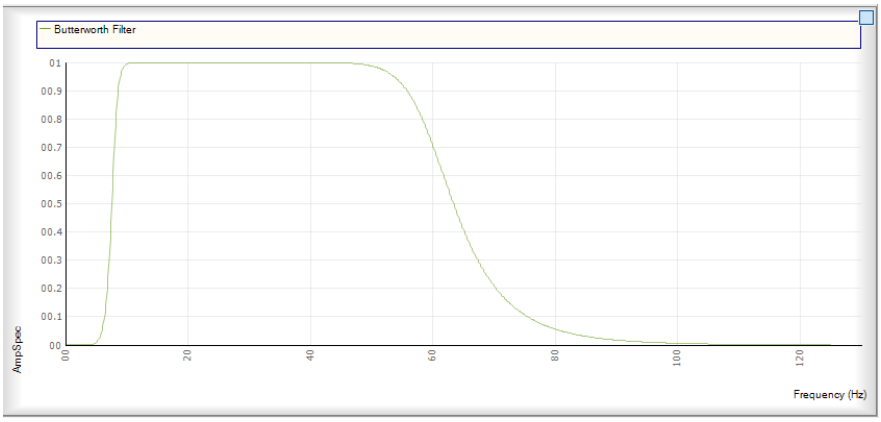

Fig (6.4): Butterworth filter.

After the process of convolution is performed, we get the seismogram (operator). There is a vast difference between the seismogram of our desire and the seismogram we obtained from the convolution.

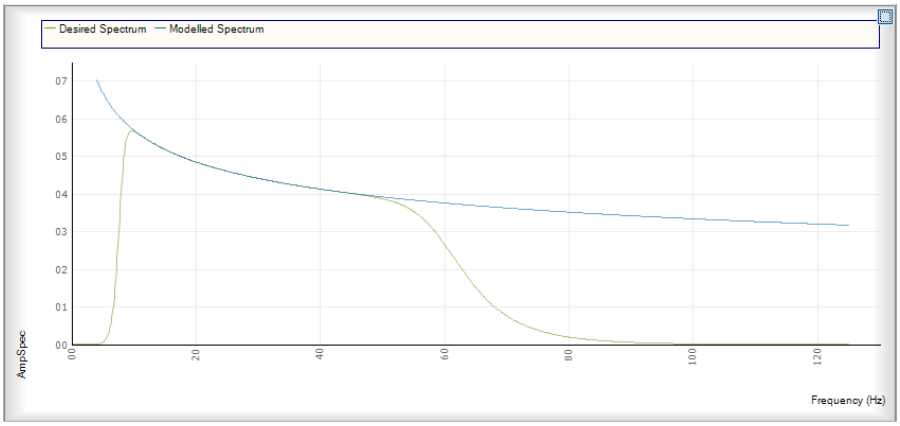

Fig (6.5): Desired and modeled spectrum.

There are two spectrums shown in figure (6.5) both are of different colors. The blue color shows the spectrum obtained from convolution of wavelet and acoustic impedance and the spectrum in blue color shows a desired spectrum. Now we need to obtain a spectrum of our desire for this purpose we have to convolve this spectrum with another spectrum known as shaping spectrum which is obtained by applying Fourier transformation on desired spectrum. The shaping spectrum is shown in figure (6.6).

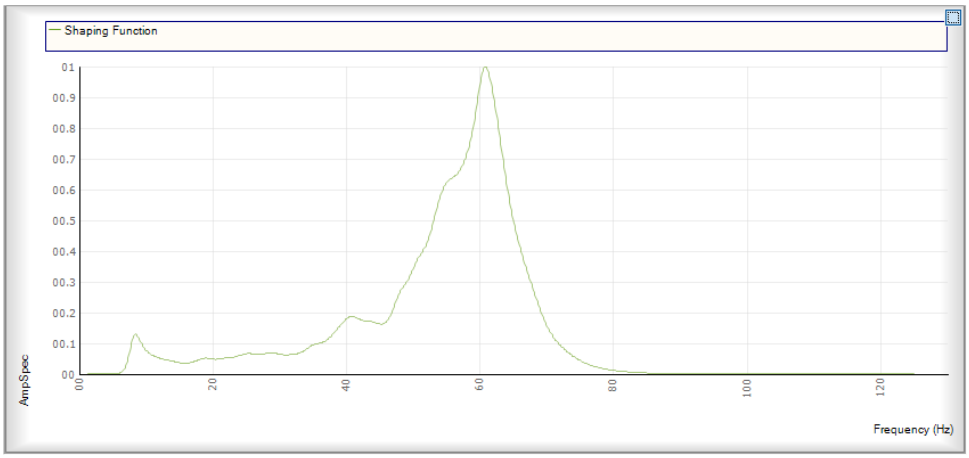

Fig (6.6): Shaping spectrum.

The figure (6.6) shows us the shaped seismic spectrum and desired seismic spectrum.

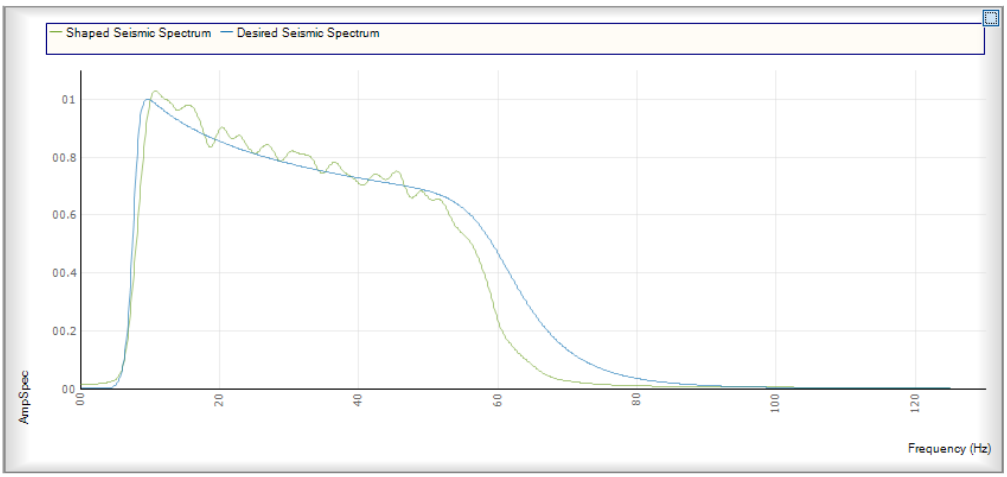

Fig (6.7): Convolution of shaped seismic spectrum and desired spectrum

A seismogram for specific window (as values of acoustic impedance is obtained from well data) is developed now we develop a seismogram to invert whole section. For this purpose, we convolve desired spectrum with seismic mean spectrum. After convolving seismogram with seismic mean spectrum, we are able to apply it on whole seismic section.

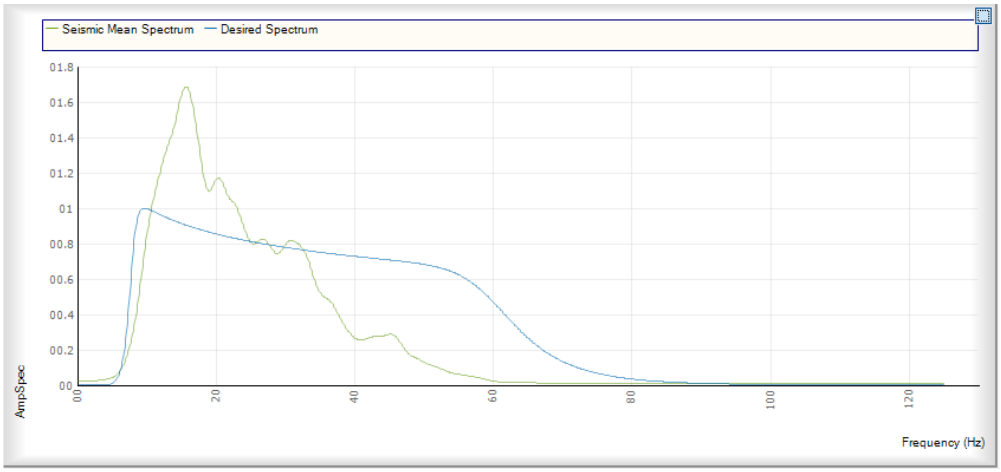

Fig (6.8): Convolution of seismic mean spectrum and desired spectrum

After completion of the process of generating synthetic seismogram, the section is inverted an acoustic impedance is shown on section instead of amplitude as shown in figure (6.9)

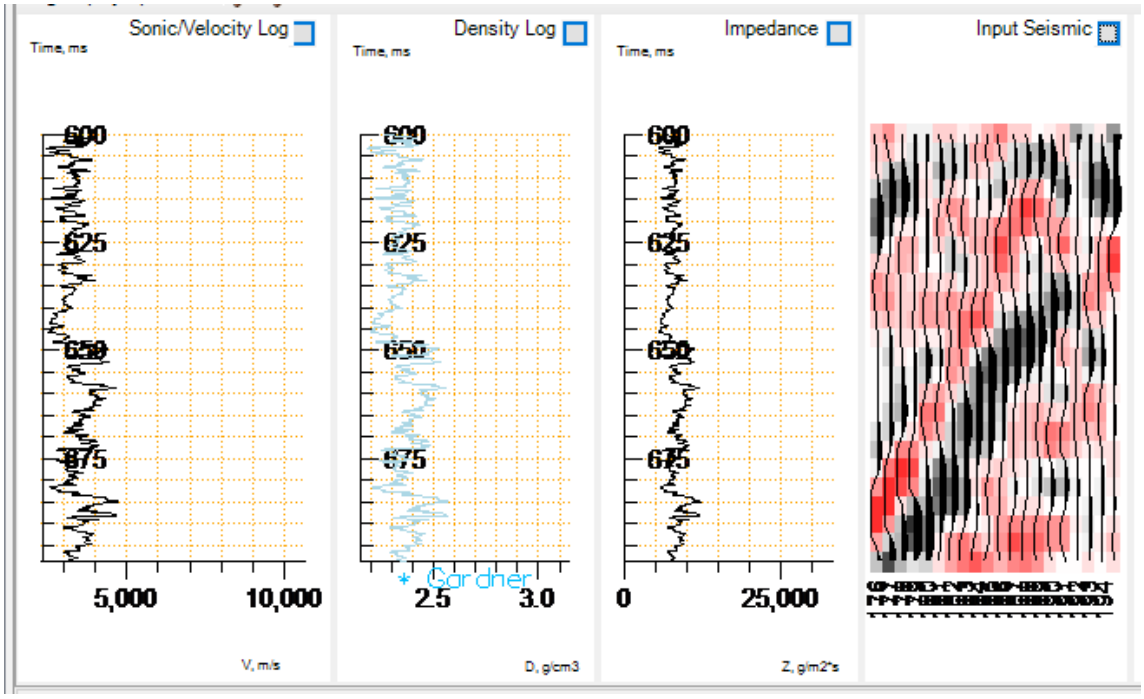

Fig (6.9): Input seismic section and inverted section along with logs.

6.7 Interpretation of Inverted Section:

After convolution of seismogram with mean spectrum an inverted seismic section is generated as shown in above figures. The inverted section can be interpreted by using

color bar. The white to yellow color shows high values of acoustic impedance and blue to green color shows low impedance.

The hydrocarbons accumulation is associated with low acoustic impedance. The given inverted section is shown with T-D chart and it shows Formations as well. The Formation circled in figure is Chorgali and Sakesar. it yields a response of low acoustic impedance it is related to presence of hydrocarbon accumulation it is also confirmed from Petrophysical results.

The Chorgali and Sakesar is interpreted as most producing reservoir in Joya Mair area. Because results obtained from seismic inversion shows low values of impedance and structure formed is anticline both conditions give indication for presence of hydrocarbons. The zoomed view of figure also confirms our results.

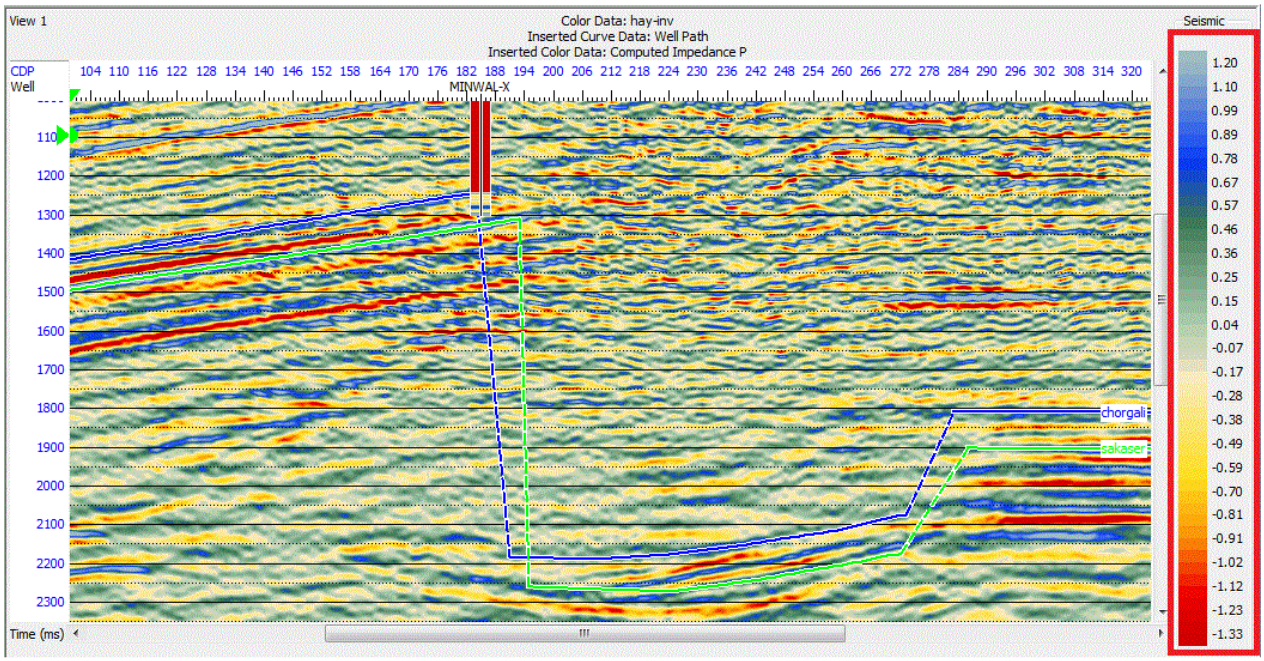

Fig 6.10 show the inverted zone

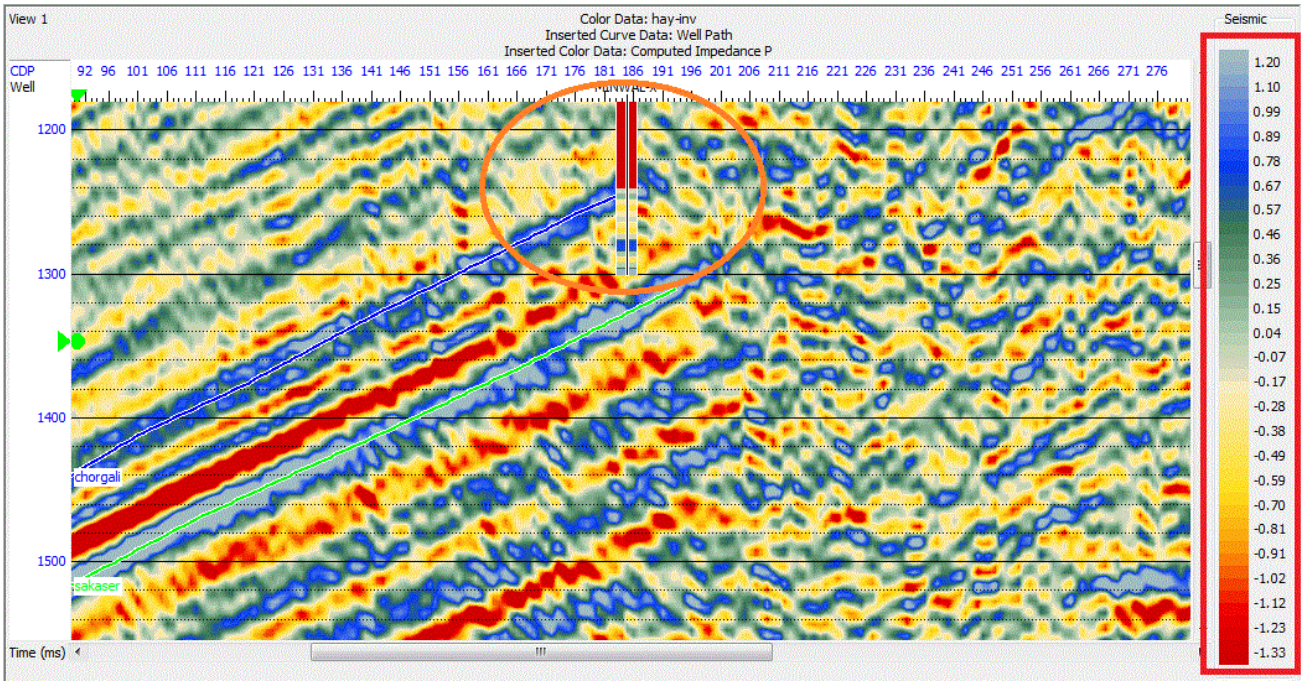

Fig 6.11 show the zoomed interested zone of seismic

6.11 Discussion and Conclusions:

- The structure of the Joya Mair oil field is recognized as triangle zone in the subsurface and an open anticline at the surface. The triangle zone is formed by the combination of thrust and backthrust. The thrust and backthrust phases are the result of northwest and southeast successive Himalayan compression.

- The thrust and backthrust of the triangle zone are found to be sealing on either side of the structure. The clays of the Rawalpindi Group act as a seal along these faults.

- The reservoir rock is Sakesar Limestone that occurs at the depth of ~2023 m interpreted from seismic data.

- The southeastern flank of the Joya Mair Triangle Zone has been exploited where the northwestern flank is untapped. It is therefore suggested that the northwestern flank of the triangle zone be drilled for further recovery of oil from the Eocene reservoir.

- From the petrophysical analysis it is clear that the Minwal X-1 well is a hydrocarbon saturated well containing an average of about 66.8% oil in its pores

spaces.

- The opposite directed thrust formed the triangle zone geometry.
- The petrophysical analysis shows that the Chorgali and Sakesar formations are the producing reservoirs in the study area.

References

Aamir, M. and M.M. Siddqui, 2006. Interpretation and visualization of thrust sheets in a triangle zone in eastern Potwar, Pakistan. The Leading Edge., 25: 24-37.

Ahmad, A. H. M., Bhat, G. M., & Khan, M. H. A. (2006). Depositional environments and diagenesis of the kuldhar and Keera Dome carbonates (Late Bathonian–Early Callovian) of Western India. Journal of Asian Earth Sciences, 27(6), 765-778.

Asquith, G. B., Krygowski, D., & Gibson, C. R. (2004). Basic well log analysis (Vol. 16). Tulsa: American Association of Petroleum Geologists.

Baker, D.M., Lillie, R.J., Yeats, R.S., Johnson, G.D., Yousuf, M., Zamin, A.S.H., 1988. Development of the Himalayan frontal thrust zone, Salt Range, Pakistan. Geological Society of America, 16, 3-7.

Banks, C. J., & Warburton, J. (1986). 'Passive-roof'duplex geometry in the frontal structures of the Kirthar and Sulaiman mountain belts, Pakistan. Journal of structural Geology, 8(3-4), 229-237.

Baranov, V., & Kunetz, G. (1960). Film synthetique avec reflexions multiples theorie et calcul pratique. Geophysical Prospecting, 8(2), 315-325.

Batzle, M., & Wang, Z. (1992). Seismic properties of pore fluids. Geophysics, 57(11), 1396-1408.

Bender, F., & Raza, H. A. (1995). Geology of Pakistan.

Berryman, J. G. (1999). Origin of Gassmann's equations. Geophysics, 64(5), 1627-1629.

Butler, R.W., Coward, M.P., Harwood, G.M., Knipe, R.J., 1987. Salt control on thrust geometry, structural style and gravitational collapse along the Himalayan mountain front in the Salt Range of northern Pakistan. In: Lerche, I., O'Brien, J.J., (Eds.), Dynamical geology of salt and related structures. Academic Press, 339-418.

Butterworth, S. (1930). On the theory of filter amplifiers. Wireless Engineer, 7(6), 536-541.

Buxton, M. W. N., & Pedley, H. M. (1989). Short Paper: A standardized model for Tethyan Tertiary carbonate ramps. Journal of the Geological Society, 146(5), 746-748.

Coffeen, J. A. (1986). Seismic exploration fundamentals.

Cooke, D. A., & Schneider, W. A. (1983). Generalized linear inversion of reflection seismic data. Geophysics, 48(6), 665-676.

Crawford, A.R., 1974. The Salt Range, the Kashmir Syntaxis and Pamir Arc, Earth and Planetary Science Letters, 22, 371-379.

Décollement Vs basement faulting. In: Farah, A., DeJong, K. (Eds.), 1979. Geodynamics of Pakistan. Geological Survey of Pakistan, 131-142.

Dobrin, M.B., Savit, C.H., 1988. Introduction to Geophysical Prospecting. McGraw-Hill Book Co., New York, 4th Edition, 1-867.

Gassmann, F. (1951). Elastic waves through a packing of spheres. Geophysics, 16(4), 673-685.

Gee, E. R., & Gee, D. G. (1989). Overview of the geology and structure of the Salt Range, with observations on related areas of northern Pakistan. Geological Society of America special paper, 232, 95-112.

Han, D. H., & Batzle, M. L. (2004). Gassmann's equation and fluid-saturation effects on seismic velocities. Geophysics, 69(2), 398-405.

Hasany, S.T., and Saleem, U., 2001. an Integrated Subsurface, Geological & Engineering

Jaume, S.C., Lillie, R.J., 1988. Mechanics of the Salt Range Potwar Plateau, Pakistan: a fold and thrust belt underlain by evaporites. Tectonics, 7, 57-71.

Jurgan, H., & Abbas, G. (1991). On the Chorgali Formation at the type locality. Pakistan Journal of Hydrocarbon Research, 3(1), 35-45.

Kazmi, A.H., and Jan, M.Q., 1997, Geology and Tectonic of Pakistan, Graphic

Khan, M. A. S. K., Radwan, T. S., & Rahman, M. A. (2006, July). Wavelet packet

transform based protection of three-phase IPM motor. In 2006 IEEE International Symposium on Industrial Electronics (Vol. 3, pp. 2122-2127). IEEE.

Khan, M. A., Ahmed, R., Raza, H. A., & Kemal, A. (1986). Geology of petroleum in Kohat-Potwar depression, Pakistan. AAPG bulletin, 70(4), 396-414.

Kozary, M. T., Dunlap, J. C., & Humphrey, W. E. (1968). Incidence of saline deposits in geologic time. Geol Soc Am Spec Pap, 88, 43-57.

Kumar, D. (2006). A tutorial on Gassmann fluid substitution: Formulation, algorithm and Matlab code. matrix, 2(1).

Malik, Z., Kemal, A., Malik, A. and Bodenhausen, J. W., 1988,

Mitra, S. (1986). Duplex structures and imbricate thrust systems: geometry, structural position, and hydrocarbon potential. AAPG bulletin, 70(9), 1087-1112.

Moghal, M. A., Saqi, M. I., Hameed, A., & Bugti, M. N. (2007). Subsurface geometry of Potwar sub-basin in relation to structuration and entrapment. Pakistan Journal of Hydrocarbon Research, 17, 61-72.

Molnar, P., Tapponnier, P., 1975. Cenozoic tectonics of Asia: Effects of a continental collision. Science, 189, 419–426.

Petroleum potential and prospects in Pakistan: International Symposium on Petroleum for the Future, Jan. 28-30, Islamabad, Ministry of Petroleum and Natural Resources.

Powell, C.M.A., Conaghan, P.J., 1973. Plate tectonics and the Himalayas. Earth and Planetary Science Letters, 20, 1-12.

publishers, Karachi, Pakistan

Rider, M. H. (2006). The geological interpretation of well logs.

Russell, B. H., Hedlin, K., Hilterman, F. J., & Lines, L. R. (2003). Fluid-property discrimination with AVO: A Biot-Gassmann perspective. Geophysics, 68(1), 29-39.

Schlumberger, 1977. Log Interpretation charts: Houston. Schlumberger well services inc. Seeber, L.J., Armbruster, J.G., 1979. Seismicity of the Hazara Arc in Northern

Pakistan:

Sen, M. K., & Stoffa, P. L. (2013). Global optimization methods in geophysical inversion. Cambridge University Press.

Shami, B.A., Baig, M.S., 2002. Geomodeling for the enhancement of hydrocarbon potential of Joya Mair field, Potwar, Pakistan. Pakistan Association of Petroleum Geoscientists-Society of Petroleum Engineers, annual technical conference, Islamabad, 124-145.

Smith, T. M., Sondergeld, C. H., & Rai, C. S. (2003). Gassmann fluid substitutions: A tutorial. Geophysics, 68(2), 430-440.

Study of Meyal Field, Potwar Plateau, Pakistan.

Swartz, C. A., Peterson, R. A., & Fillippone, R. W. (1955). Synthesis of Seismograms from Well Log Data. The Journal of the Acoustical Society of America, 27(1), 199-199.

Vail, P. R., & Mitchum Jr, R. M. (1979). Global cycles of relative changes of sea level from seismic stratigraphy: resources, comparative structure, and eustatic changes in sea level.

Velzeboer, C. J. (1981). The theoretical seismic reflection response of sedimentary sequences. Geophysics, 46(6), 843-853.

Wang, Z. (2001). Fundamentals of seismic rock physics. Geophysics, 66(2), 398-412.

Zaidi, S. N. A., Brohi, I. A., Ramzan, K., Ahmed, N., Mehmood, F., & Brohi, A. U. (2013). Distribution and hydrocarbon potential of Datta sands in Upper Indus Basin, Pakistan. Sindh University Research Journal-SURJ (Science Series), 45(2).